CALCULATION OF STRONG GROUND MOTION AND LOCAL FIELD - FAR FIELD RELATIONSHIPS FOR THE APRIL 25, 1965, PUGET SOUND, WASHINGTON, EARTHQUAKE

Dr. Charles A. Langston

Pennsylvania State University
University Park, Pennsylvania

USGS CONTRACT NO. 14-08-0001-18235
Supported by the EARTHQUAKE HAZARDS REDUCTION PROGRAM

OPEN-FILE NO.81-377

U.S. Geological Survey
OPEN FILE REPORT

Table of Contents

Introduction

Work related to this contract has concentrated in producing viable source models for the April 1965 Puget Sound earthquake and viable earth structure models for Puget Sound and nearby areas to study the effects of strong ground motion wave propagation. Several different yet related topics have been addressed in this study. These are:

1. Construction of both deterministic and empirical source models for the 1965 Puget Sound earthquake based on teleseismic body wave data;

2. Investigation of crustal and upper mantle structure under specific sites in the Pacific Northwest;

3. Calculation of strong ground motions using these source and structure models with comparison to existing strong motion data recorded from the 1965 event.

Technical Discussion - Part I:

"A Study of Puget Sound
Strong Ground Motion"

(to be submitted to the Bulletin of the
Seismological Society of America)

Abstract

An attempt was made to model observed strong motion velocities and displacements from the April 29, 1965, magnitude 6.5 Puget Sound earthquake. Several different plane layered crustal models were assumed based on previous seismic refraction measurements. Source parameters for the 1965 event were taken from a previous study of teleseismic body waves. Teleseismic P waves recorded at Tumwater, Washington, near the Olympia strong motion site, were examined to place constraints on allowable interface contrasts and to determine whether lateral heterogeniety is a major factor affecting wave propagation. Because of the 60 km source depth and close epicentral distances for the strong motion sites, it proved adequate to approximate ground displacements and velocities by assuming an impinging P or S plane wave under the various crustal models and using a propagator matrix technique to compute the response. Amplitudes were scaled using the generalized ray theory result for direct P, SV, and SH waves from a point dislocation. Although strong motion models qualitatively showed many of the characteristics of near-vertical wave propagation in layered structures, the observed amplitude behavior of individual stations was quite complex. Data from Tacoma and Seattle sites, close to the epicenter, attained lower velocities and acceleration compared to Olympia which was three times as far. The amplitude behavior is consistent with higher attenuation under Tacoma and Seattle although this is not strictly required. The short-period P data recorded at Tumwater showed evidence of large

velocity contrast interfaces under the station, from large P to S conversions, consistent with those assumed in the crustal models. Comparison of both horizontal components for several teleseisms also indicated that dipping structure or other lateral heterogeniety is important for Olympia structure. Thus, it is likely that strong motion amplitudes and waveshapes are also controlled by scattering mechanisms to a large degree. Irrespective of these wave propagation problems, the largest single factor which has affected the level of strong ground motions in Puget Sound is the large source depth of past earthquakes. Using a simple geometrical spreading argument it is shown that if the 1965 event was only at 10 km distance from Olympia instead of 100 km, all other effects being equal, then greater than 1g accelerations would have been recorded. Thus, estimates of seismic hazard based on a direct interpretation of the strong motion data of the 1965 and 1949 events will be erroneously biased towards less hazard if there is potential for shallow faulting in the Puget Depression.

Introduction

According to studies of historical seismicity (Algermissen, 1969; Milne, 1967; Howell, 1974), the Puget Sound area is one of high seismogenic potential and hazard, yet little is known of the geologic and geophysical factors which influence earthquake occurrence and resulting strong ground motions. The purpose of this paper is to investigate characteristics of strong ground motion recorded from the April 29, 1965, earthquake in an attempt to sort out factors important to wave propagation in the Puget depression. Recent work involving deterministic modeling of earthquake strong motions from shallow depth sourced has shown promise in estimating the effects of source when close to the source (e.g., Heaton and Helmberger, 1979) or in estimating structure effects on wave propagation when source parameters are known (Heaton and Helmberger, 1977; 1978). These studies have been most successful when modeling assumptions agree closely with the natural structure and when the long period band (e.g., displacements) is examined.

Because of limitations imposed by the relatively sparse strong motion data set and lack of geophysical control over small scale structures in Puget Sound, this study will necessarily be one of determining general characteristics of strong-motion wave propagation in southern Puget Sound within a deterministic framework. For example, a major purpose here is to determine whether plausible plane layered earth models can reproduce the duration and amplitude behavior of observed ground velocity from the 1965 event. Constraints on the source time function, orientation, and depth for the 1965 event are available from a study of teleseismic P and S

waves (Langston and Blum, 1977). Gross constraints on earth models are available from travel time and refraction studies (Crosson, 1976; Zuercher, 1975). Further, because of the fortuitous location of Tumwater station (TUM) near the Olympia strong motion site, assumptions regarding the homogeniety of earth structure can be tested directly by examining teleseismic P wave forms for off-azimuth arrivals and phase conversions (Langston, 1977). Once a set of earth and source models is produced for the 1965 event, they can then be evaluated for implications involving other assumed sources.

The 1949 magnitude 7.1 event and the 1965 magnitude 6.5 event were significant in size yet produced rather low accelerations and damage compared to like magnitude events in Southern California (Algermissen et al, 1965; Mullimeax et al, 1967). Their unusually large depths (70 and 60 km, respectively) will be shown to be the largest single factor in explaining these observations. Thus, it may be that the greatest problem in evaluating seismic risk in Puget Sound concerns not the effects of similar deep events but the effects of possible shallow, near surface, faulting.

Structural Setting

Algermissen et al (1965), Crosson (1972), and Langston and Blum (1977) give several general and topical descriptions of the geology and tectonics of the Puget Sound region. Of primary interest here are the characteristics of crustal structure in the Puget depression. The early pioneering refraction work of Tatel and Tuve (1955) indicated that the crust was rather thin in

Southern Puget Sound, having Moho depths of only about 20 km. Subsequent refraction work by Berg et al (1966) in the Oregon Coast Ranges and by Zuercher (1975) in Southern Puget Sound and the Olympic Peninsula confirm this shallow Moho depth. However, crustal structure studies in central Puget Sound based on earthquake travel time residuals (Crosson, 1976) and unreversed refraction (Zuercher, 1975) indicate that the Moho may be depressed by as much as 15 km obtaining 35 km depths. Indeed, Zuercher (1975) showed that crustal thicknesses and upper crustal velocities may vary considerably in Puget Sound. Implied dips from his structure interpretation may be as great as 45°.

Gravity and magnetic studies also indicate considerable variation in large scale crustal structures. Danes̆ et al (1965) proposed a northwest-southeast horst structure trending through the center of Puget Sound with flanking deep sedimentary basins. The unconsolidated sediment thickness map compiled by Hall and Othberg (1974) mimics Danes̆' structure and shows greater than 1 km sediment thicknesses under Seattle and Tacoma (see Figure 1 also). Gradients in the thickness are very steep in places, especially near Seattle.

An indication of the nature of short period (1 hz) wave propagation in Puget Sound was obtained in a study of teleseismic pP from the April 1965 event by Langston and Blum (1977). They noticed a dramatic amplitude reduction in short period pP, relative to direct P, even for stations where P was nodal and long period pP was several times larger than direct P. The absence of short period pP seemed to correlate with sediment thickness at its reflection point. An effective Q of 65 was inferred for the structure

between the hypocenter and surface although the amplitude depletion may have been due to scattering as well.

Thus, from all indications, the crustal structure of Puget Sound appears to be heterogeneous and profoundly affects short period wave propagation. The analysis of strong motion data and teleseismic body wave data will show that these heterogenities are probably significant in shaping wave forms and amplitudes although many of the general characteristics in the data can be explained by plausible crustal models.

Strong Motion Data from the 1965 Event

Three-component strong-motion acceleration data were recorded at three locations within Puget Sound from the 1965 earthquake (Figure 1). Additionally, the Tacoma and Seattle sites contained Carder displacement meter instrumentation which recorded horizontal motion. Table 1 lists the station locations, distances and azimuths from USCGS and ISC epicenters for the 1965 events. Table 2 displays instrumentation parameters. Corrected accelerogram data for the Olympia site was obtained in digital format from the Earthquake Engineering Research Laboratory of California Institute of Technology. Techniques and errors involved in processing these data are described by Trifunac et al (1973) and Trifunac and Lee (1974). Analogue copies of the acceleration and displacement meter recordings at Tacoma were obtained from the Solid Earth Data Center in Boulder, Colorado, since these were unavailable in digital form. Further, the Seattle data were unavailable from both sources and were obtained from high quality reproductions displayed in Algermissen et al (1965). The analogue data were

manually digitized at an uneven time increment and then interpolated to an equal time spacing of 0.01 seconds. The data were then corrected for instrument responses and band-passed filtered to remove baseline and digitizing noise. Amplitudes above 25 hz and below 0.05 hz were removed to be consistent with the Ormsby filtering operation described by Trifunac et al (1973). Acceleration and velocities were computed from the accelerogram data and velocity and displacement computed from the Carder displacement meter data. Figures 2, 3, and 4 display the processed accelerogram data for Olympia, Seattle, and Tacoma, respectively. Figures 5 and 6 display the processed Carder displacement meter data for Seattle and Tacoma, respectively.

Consistency between wave shapes for ground velocities derived from the acceleration and Carder data is generally good except for Tacoma NS components; the Tacoma NS Carder data was low amplitude and more difficult to digitize. Velocity amplitudes derived from the Carder data are also about 20% lower than those derived from the acceleration data. This is consistent with differences observed in comparisons of other similar data made by Trifunac and Lee (1974) and Heaton and Helmberger (1977) and is probably due to slight instrument miscalibration.

The acceleration data of Figures 2, 3, and 4 are very similar in form to local earthquake recordings. Indeed, there is no reason to treat them other than high-amplitude local earthquake seismograms. For example, in Figure 4 the vertical component appears to have an initial 'P' arrival and after about 5 seconds,a later 'S' arrival. This is more apparent in

the horizontal components where the S arrival at about 6 to 7 seconds into the record is several times larger than the first arrival. Tacoma is only about 20 km from the epicenter (Table 1) and the source is 60 km deep. This implies an S-P time of about 7 seconds which is consistent with the S- trigger time observed in Figure 4. Further, since the receiver is directly above the hypocenter, incident angles should be steep. P waves should be largest on the vertical component and S waves should predominate on the horizontal components. Indeed, this is the case for all three recording sites.

The vertical and EW velocities for Tacoma are particularly simple consisting of a prominent double pulse (Figure 4). Displacements (Figure 6) show a show a prominent S wave pulse polarized entirely westward. Although velocities for Seattle (Figures 3 and 5) are somewhat more complicated than Tacoma, displacements (Figure 5) again show a relatively simple S pulse. Seattle is at approximately the same distance from the epicenter as Tacoma (Table 1), so it might be expected that the observations should be qualitatively similar.

Olympia accelerations show apparent anomalous amplitude behavior (Figure 2). Compared to Seattle, horizontal accelerations are approximately a factor of two larger at Olympia. The difference between Olympia and Tacoma is even more striking, being a factor of 3 to 4. The difference in velocity amplitudes is less striking. Figures 2, 3, and 4 also clearly show that Olympia horizontal accelerations are enriched in high frequencies compared to Tacoma and Seattle. Since Olympia is further from the source

(~70 km) these observations suggest that attenuation may play an important role in local wave propagation under the Tacoma and Seattle sites. This will be discussed in a later section.

Teleseismic Data Recorded at Tumwater, Washington

There are several particular structural properties which are of direct interest to the study of strong ground motions. First, we wish to know the nature of velocity and density contrasts under specific strong motion sites which affect wave propagation in the frequency band of about 1 to 10 hz. Observations concerning the extent and magnitude of lateral heterogeniety are also crucial since there must be a check on the validity of assumptions made in any wave calculations using simple plane-layer models. Through fortuitous circumstances, the University of Washington has been operating a three-component short-period seismic station at Tumwater, Washington (TUM). TUM is located only a few kilometers from the Olympia strong motion site (see Figure 1). Proper analysis of teleseismic body wave data recorded at TUM may therefore yield independent insight into structure appropriate for Olympia.

The basic approach in deducing structure under TUM is to compare the three components of ground motion for an incident teleseismic P wave. Because incident angles within the mantle for teleseismic rays are only 10^{o} to 20^{o}, P to S conversions from boundaries under the station will be predominent on the horizontal components and can be seen directly through comparison with the vertical component (Burdick and Langston, 1977). The relative amplitudes of these conversions indicate velocity contrast and their timing, layer

thickness. Further, a comparison of both horizontal components can be used to determine whether the structure is laterally homogeneous or not (Langston, 1977). In a system of isotropic plane layers horizontal motion due to an incident P plane wave should be polarized in the radial direction only. In the presence of layer dip or other lateral heterogeniety, side refractions and S wave polarization angle changes at reflection and transmission will cause tangential ground motions as well. This will give rise to dissimilar waveshapes for observed horizontal components. A simple glance at the data can therefore reveal whether structure under the station is laterally heterogeneous.

With these techniques in mind, data from several teleseismic events recorded at TUM station were obtained from the University of Washington. Data for three events were chosen and digitized on the basis of high signal-to-noise ratio and simplicity of the P pulse on the vertical component. This last criterion is important since effective source function complexities may mask later arriving P-to-S conversions (Burdick and Langston, 1977). Table 3 lists the teleseismic events digitized in this study and instrument characteristics for the three components at TUM. Figure 7 displays the wave form data. Table 3 indicates that the horizontal instruments are nominally matched but are slightly longer period than the vertical. Also, the gains between vertical and horizontal instruments are radically different. Some compensation for the gains was obtained by dividing the data by the stated magnification. This correction is undoubtably in error, however, since the gains in Table 3 are only approximate (Norman Rasmussen, personal communication, 1979). The vertical-to-radial amplitude ratios displayed on

Figure 7 show unrealistic values indicating that there are problems with instrument calibration. Considering the ray azimuth of approach polarities of the initial P pulse are also inconsistent for the NS and EW components for the 12-27-67 and 7-25-68 events, respectively. Nevertheless, these amplitude problems do not mask the large differences in waveshape seen between horizontal and vertical components. The 12-27-67 event displays a very simple two-second duration pulse on the vertical component followed by virtually no other arrivals for the remainder of the recording (Figure 7). The horizontal components, however, show several major P to S conversions after the initial P wave arrival. Two of the clearer arrivals are indicated by arrows. Note also that the second marked arrival on the NS component is conspicuously absent from the EW component. This is a clear indication that lateral heterogeniety is a contributing factor in shaping short period wave forms. Data from the other two events also show high relative amplitude Ps arrivals on the horizontal components and gross differences in wave shapes between the horizontal components. Thus, we can conclude from this qualitative examination of the teleseismic data that there must be one or more high velocity contrast interfaces in the upper crust under TUM and that these structures are likely to be dipping or otherwise laterally heterogeneous.

Strong Ground Motion Modeling

Although there is direct evidence from the teleseismic data that lateral heterogeniety is significant for short period wave propagation in Puget Sound, we will approach the problem of computing strong ground motions by first assuming simple plane-layered models. Other than being more

computationally tractable and efficient, plane-layered models can yield important physical insights on the major effects of structure on wave propagation.

Figure 8 displays several earth models that were assumed for wave calculations. P wave velocities for models M1 and M2 were taken from Zuercher (1975) and S wave velocities were computed assuming a Poisson solid. Densities are also assumed but are based on empirical velocity-density relations. The variation in crustal thickness for Puget Sound was the basis for assuming thickness variation between models M1 and M2. Model M3 was constructed to introduce plausible velocity variations and more wave complications to compare with the simplier models M1 and M2. In the computations to be presented, two more earth models designated M1-A and M2-A, were used to evaluate the effect of the thick unconsolidated sedimentary section. These were constructed by adding a one kilometer thick layer of low velocity material (V_p=3.0 km/sec, V_s=1.5 km/sec, ρ=2.0 gm/cm^3) to the tops of model M1 and M2, respectively.

The relatively unusual circumstance of having all three strong motion sites within the distance of one source depth from the epicenter allows a significant simplification on how wave responses may be computed. Generally, for these types of studies involving shallow sources, the response due to a point source or collections of point sources is calculated using generalized ray theory, mode theory, or wave number integration techniques. Wave propagation from shallow sources to nearby receivers is often quite complicated involving diffracted waves and surface waves. Hence, a rather

robust method is needed for their computation. For Puget Sound strong motion calculations it proved adequate to simply assume a plane wave with the appropriate ray parameter impinging on the crustal model from below. Figure 9 demonstrates that there are minor differences between responses computed using generalized ray theory (Helmberger, 1974; Langston and Helmberger, 1975) and responses computed using the simple propagator matrix formulation of Haskell (1960, 1962). Model M1 was assumed for the calculations of Figure 9 for the Olympia strong motion site (Table 1). The generalized ray calculation involved summing 47 rays for the radial component and 18 for the tangential. A 60 km depth dislocation point source with the orientation derived by Langston and Blum (1977) was also assumed (Table 1). The Haskell response was computed assuming the ray parameter for the direct S wave. All impulse responses were convolved with the velocity time function, V(t), shown in Figure 10.

The major differences between the two kinds of calculations lie principally in geometric spreading changes for converted waves such as Sp. The difference in ray parameter between rays is of little importance because of the small incident angles involved. Besides being computationally inexpensive, the propagator matrix formulation also has the advantage of naturally including all rays within the structure, an important limitation of generalized ray theory in this study. The differences in responses become less as the epicentral distance decreases. Note that this approximation is only valid because source depth is large compared to epicentral distances and typical wave lengths.

For sake of clarity in understanding the theoretical effects of structure on wave propagation, a simple velocity time function was assumed based on the

far-field time function inferred by Langston and Blum (1977). Figure 10 displays a smoothed version of their far-field time function, S(t) and its derivative, V(t). Because of the 60 km source depth and the high frequencies considered, the seismic response is dominated by far-field terms so that displacements may be computed by

$$u_i(t) = S(t) * E_i(t) \qquad (1)$$

where $u_i(t)$ is the ith displacement component and $E_i(t)$ is the structure impulse response for the ith component. Ground velocity $v_i(t)$ will therefore be

$$v_i(t) = V(t) * E_i(t) \quad . \qquad (2)$$

This, of course, assumes a point dislocation source; directivity effects are ignored here.

Figure 11 displays theoretical velocity ground motions for the Olympia site assuming incident P and S waves under the different crustal models of Figure 8. All amplitudes have been normalized depending on incident wave type and displacement component. Radial velocity responses due to an incident P wave have been normalized to the P vertical component and vertical responses due to an incident SV wave have be normalized to the radial. All SH responses have been normalized. To obtain absolute velocity (or displacement) each component is scaled to the amplitude expected for the direct ray. For example, after Langston and Helmberger (1975), the high frequency radial response, q(t) for the direct SV wave is given by

$$q(t) = \frac{M_o}{4\pi\rho_o} \frac{\sqrt{p}}{\eta_\beta} \frac{R(p)\, R_{sr}}{(-2 \frac{d^2t}{dp^2})^{\frac{1}{2}}} \sum_{j=1}^{3} A_j(\theta,\delta,\lambda)\, SV_j \quad V(t) \qquad (3)$$

where,

$R(p)$ = product of generalized reflection and transmission coefficients

R_{sr} = radial SV wave receiver function

$A_j(\theta,\delta,\lambda)$ = horizontal radiation pattern coefficients

SV_j = SV wave vertical radiation pattern coefficient.

p = ray parameter

M_o = seismic moment.

Definitions of these and other parameters may be found in Helmberger (1974) and Langston and Helmberger (1975).

Vertical P waves and tangential SH waves are relatively unaffected by structure, having only minor reverberations occurring after the major direct arrival. Radial P shows many large P to S conversions and reverberations from the interfaces in the earth models. Radial SV shows a long coda of waves which are about 25% the amplitude of the large direct SV pulse. The vertical SV response rings a great deal but is only 20% to 30% the amplitude of the vertical. The extreme ringing in the vertical SV response is due to trapped S to P conversions within the crustal model. The ray parameter for incident S waves is greater than 1/8 sec/km so that converted S to P waves have greater than critical incident angles at the lowermost boundary in all models. Note that all models give similar results and that

effect of including low velocity sediments (models M1-A and M2-A) serves only to increase the coda in the radial P and vertical SV responses somewhat. Inclusion of more layer interfaces (model M3) also does little to increase complexity. Returning to the Olympia strong motion data, Figure 2, we see that these models are in qualitative agreement with the observations. The vertical component shows smaller S packet amplitudes (20% to 30%) relative to the horizontals, and is of longer duration with considerable ringing. The complexity of the observed horizontal components may be partially explained by appealing to a more complicated velocity function but this probably can't explain the relatively long codas of each.

Synthetics appropriate to the Tacoma and Seattle sites are shown in Figure 12. Wave effects are similar to those in Figure 11 except that incident angles are steeper for these close stations. There are also no critical angles for S to P conversions which dramatically reduces the ringing in both radial and vertical SV wave responses. This kind of behavior is qualitatively reflected in the Tacoma data of Figure 4. The S pulse seen in the EW component is relatively simple with little later reverberations. The S wave arrival on the vertical component is very small and comparable to the large radial/vertical SV wave amplitude ratio seen in Figure 12. The SN component, however, shows low amplitudes, which is probably an artifact of S polarization angle, but a long duration coda. This coda is undoubtably a result of scattering not unlike that seen in the teleseismic P wave data.

The velocities at Seattle (Figure 3) are much more complex than those at Tacoma and certainly more complex than those of the models in Figure 12.

Although some of this may be due to the seismic source function there is indirect evidence from displacement amplitudes, presented in a later section, that severe scattering may be occurring under the Seattle site.

Figure 13 presents a suite of synthetic seismograms for the teleseismic P data recorded at TUM. A two-second duration pulse similar to that of the 12-27-67 event (Figure 7) was convolved with earth responses calculated for each model. Although this calculation is only approximate, considering the evidence for lateral heterogeniety in the teleseismic data, it nevertheless should be adequate to determine whether the large velocity contrasts in the upper parts of the earth models are reasonable or not. Calculations of responses in moderately dipping structures indicate that tangential component waveshapes are most affected by the structure but that the radial usually only changes in detail (Langston, 1977). Since tangential motions are usually smaller than radial, horizontal motions composed of both should also be largely unaffected especially in the beginning portions of the records. Figure 13 shows that later arriving P to S conversions in the radial component do indeed attain amplitudes comparable to those seen in the data of Figure 7. In fact, model M2, which should be most appropriate for TUM, shows relative amplitude, waveshape, and timing behavior which is nearly identical to the first 15 records of the 12-27-67 data. This is a remarkable and heartening result since models M1 and M2 were constructed a priori from the refraction results of Zuercher (1975).

Strong motion velocity and displacement amplitudes were computed using the orientation and seismic moment determined by Langston and Blum (1977) (Table 1) and the time functions displayed in Figure 10. The maximum

amplitude of each velocity trace is compared to its expected value in Table 4. Amplitudes for displacements are taken from the height of the observed and calculated S wave pulse. Because the S wave responses in Figure 12 primarily show only the direct wave the displacements are nearly identical to the time function, S(t) (Figure 10). They are therefore not shown. The USCGS epicenter was assumed for the station-source geometry. Using the ISC epicenter changes these amplitudes by only 20%. Acceptable variations in the source mechanism can also affect individual amplitudes by as much as 50% but the vector sum of direct S amplitudes usually changes only $\pm$20%.

The expected large horizontal velocities at Tacoma and Seattle are most variant with the data. In the model, these are largely controlled by source orientation where the stations are near maxima in the SH wave radiation pattern. This is little affected by plausible and allowable variations in the dip of the auxilliary plane of the focal mechanism since each station is directly above the source and the inferred fault plane is nearly vertical. Although the velocity time function is oversimplified it is not likely that directivity effects could cause such a difference in amplitudes. The primary evidence for this comes from the previous study of teleseismic P waves (Langston and Blum, 1977). It was observed that although short-period pP was attenuated relative to direct P for some data, short-period pP and sP were readily apparent for stations further from the source. Body waves for these stations had near vertical incidence angles. Thus, the large changes in amplitude observed for pP could not be explained by directivity models since these changes were occurring over ray angle changes of only about 10^{o}.

Other evidence for near receiver structure affecting these strong motion amplitudes comes from the comparison of displacements for Seattle

and Tacoma (part B, Table 4). Although Seattle model displacements are reasonable in terms of amplitude, the model fails to predict the polarity of the S58°W S pulse (see also Figure 5). This polarity is mainly a function of the large SH wave predicted by the radiation pattern and cannot be changed by any reasonable manipulation of the source mechanism. Instrument polarity is probably not to blame since velocities computed using the Carder and accelerometer data agree (Figures 3 and 5). Thus, this polarity reversal represents a major deficiency in the model and may be due to extreme lateral heterogeniety in the structure at Seattle. The predicted S wave at Tacoma is about three times larger than observed and its polarization angle allows too much displacement on the NS component. As in the case of predicted velocities and observed accelerations, Tacoma again exhibits lower than expected amplitudes.

Discussion

The preceding modeling experiments all point to the conclusion that several underlying assumptions on earth structure and, perhaps, source mechanism must be grossly inadequate. Taken individually, data at each station exhibit characteristics expected for near-vertical wave propagation in layered structures. However, the general observation that the closer stations have smaller amplitudes than the further station is contradictory to all intuition and modeling. If we take the factor of 5 discrepancy between observed and calculated velocities at Tacoma to be true and appeal to an attenuation mechanism to reduce the model velocities, a Q of about 28 is obtained for a one hertz S wave traveling along the entire path between

the hypocenter and station. This qualitatively agrees with the effective Q_α of 65 obtained from teleseismic pP attenuation for the Puget Sound event (Langston and Blum 1977). If the attenuation is confined within the upper layers of the crust and, in particular, the thick sediments under Tacoma or Seattle, then exceptionally low values are obtained (~1). These low Q values would not explain the same factor of 5 difference between 5 to 10 hertz accelerations at Olympia and Tacoma, however, unless Q was frequency dependent. In any case, since there is little to constrain the high frequency portion of the source spectrum, it can only be said that the amplitude discrepancies between stations and between models and data are consistent with higher attenuation under Seattle and Tacoma relative to Olympia.

In a recent comparative study of strong ground motion from the 1965 and 1949 Puget Sound events, Shakal and Toksoz (1980) suggest that attenuation is a major factor in wave propagation under the Seattle site compared to Olympia. They make this claim on the basis of low accelerations consistently observed at Seattle between both events. Although this type of model is supported here by the data and amplitude discrepancies between model and data, a further independent study is needed to definitively prove this. If there is an equal chance that the amplitude effect is due to source directivity or receiver structure attenuation, for each event, then there is a 1 in 4 chance that the observed effect is due to directivity rather than attenuation. A detailed study of teleseismic sources recorded at several broad-band stations in these areas of Puget Sound could answer this important question.

The results of this study fall considerably short of goals desired in most wave form studies. The anomalies observed between data and synthetics are partly due to the inadequacies of the source time history which was assumed. However, the large differences in amplitude and even polarity between observe and calculated displacements are particularly bothersome since they are caused by stable aspects of the model. Tacoma and Seattle are close to the source and amplitudes should be dominated by the maximum of the SH wave radiation pattern. On the basis of past seismic, gravity, and magnetic studies of crustal structure in Puget Sound and on the basis of the qualitative analysis of teleseismic P wave forms at TUM, it does seem clear that lateral heterogeniety is probably the major factor in these anomalies. Further work into wave propagation in Puget Sound should be performed to map out these heterogenieties in detail. One particularly simple method would be to use the P particle motion recorded from teleseismic sources on a dense broad-band three-component array. The analysis of off-azimuth arrivals could yield considerable information to the nature of velocity discontinuities , including layer dip and velocity contrasts, below the station. Thus type of information is indispensable to understanding ground motions from local earthquakes.

Irrespective of discrepant details, some order-of-magnitude estimates can be made concerning the gross characteristics of strong ground motion in Puget Sound. For example, even if the Olympia acceleration data are considered (Figure 2), it is evident that maximum accelerations were relatively low for a magnitude 6.5 earthquake. A maximum of only about 0.2g is observed compared to the greater than 1g accelerations observed at some stations for

the 1971 San Fernando earthquake or the 1979 Imperial Valley earthquake. The major difference between the 1965 event and these other events is depth. If it is reasonably assumed that the 1965 accelerations are dominated by body waves then they may be approximately corrected back to a point near the source using geometrical spreading. If the source was 10 km from Olympia rather than about 100 km, accelerations could have been as high as 2g using this simple technique. Figure 14 displays acceleration and velocities recorded at Olympia for the 1949 event. This event occurred at 70 km depth (Nuttli, 1952) and shows acceleration slightly larger than observed for the 1965 event. If the source was shallower at 10 km rather than 70 the geometric spreading correction again gives values greater than 2g. Although this is an approximate analysis, it does indicate that the level of strong ground motion in Puget Sound has, in the past, been controlled by large source depths rather than low intensity source radiation.

Second order wave propagation considerations, such as attenuation or lateral heterogeniety, may therefore be moot to the true seismic hazard of Puget Sound. The past strong ground motion record of Puget Sound is probably biased on the low side because of previous large source depths. Shallow earthquakes with possible surface or near-surface faulting may well overshadow the destructive effects of past historical events in the Puget Depression. Although the late Quaternary sedimentary cover in the area has hampered seismotectonic studies of near surface faulting, there is evidence that recent shallow faulting near the eastern Olypmic mountains has occurred (Wilson, et al 1979) and may well be currently active.

Conclusions

The general behavior of observed strong motion velocities and displacements from the 1965 Puget Sound earthquake can be explained by near-vertical body wave propagation in plausible plane-layered crustal models. Some aspects of the data are poorly modeled, however. The lower velocity and displacement amplitudes observed at Tacoma and Seattle, relative to Olympia, are contrary to the synthetic calculations and physical intuition. The amplitude behavior is suggestive of high attenuation under Tacoma and Seattle.

Short-period teleseismic body wave data recorded nearby at Tumwater, Washington show large P to S conversions consistent with assumed crustal structures. They also show large off-azimuth P to S arrivals which indicate substantial deviation from plane-layered models. In conjunction with past geologic and geophysical studies, these data then suggest that scattering may play an important role in local wave propagation.

The largest single factor which has controlled past strong ground motion levels in Puget Sound is source depth. Large shallow earthquakes may be expected to be associated with significantly larger accelerations than previously experienced in Puget Sound in accordance with shallow events elsewhere.

Acknowledgments

I would like to thank Norman Rasmussen of the University of Washington for his kind assistance in procuring the data for Tumwater station and Walter Arnold for his help in processing the digital strong motion data. This research was supported by the U.S. Department of the Interior, Geologic Survey, under contract No. 14-08-0001-18235.

REFERENCES

Algermissen, S. T. (1969). Seismic risk studies in the United States, Proc. 4th World Conf. Earthquake Eng., p. 1-20.

Algermissen, S. T., S. T. Harding, K. V. Steinbrugge, and W. K. Cloud (1965). The Puget Sound, Washington earthquake of April 29, 1965, U.S. Department of Commerce, Coast and Geodetic Survey, Rockville, Maryland.

Crosson, R. S. (1972). Small earthquakes, structure, and tectonics of the Puget Sound region, Bull. Seismol. Soc. Am. 62, 1133-1171.

Crosson, R. S. (1976). Crustal structure modeling of earthquake data 2. Velocity Structure of the Puget Sound region Washington, Jour. Geophys. Res., 81, 3047-3054.

Danes, Z. F., M. M. Bonno, E. Brau, W. D. Gilham, T. F. Hoffman, D. Johansen, M. H. Jones, B. Malfair, J. Masten, and G. O. Teague (1965). Geophysical investigation of the Southern Puget Sound area, Washington, Jour. Geophys. Res. 70, p. 5573-5580.

Hall, J. B. and K. L. Othberg (1974). Thickness of unconsolidated sediments, Puget lowland, Washington, Geologic Map GM-12, State of Washington Department of Natural Resources, Olympic, Wash.

Haskell, N. A. (1960). Crustal reflection of plane SH waves, Jour. Geophys. Res., 65, p. 4147-4150.

Heaton, T. H. and D. V. Helmberger (1977). A study of the strong ground motion of the Borrego Mountain, California, earthquake, Bull. Seismol. Soc. Am., 67, p. 315-330.

Heaton, T. H. and D. V. Helmberger (1978). Predictability of strong ground motion in the Imperial Valley: Modeling the M 4.9, November 4, 1976 Brawley earthquake, Bull. Seismol. Soc. Am., 68, p. 31-48.

Heaton, T. H. and D. V. Helmberger (1979). Generalized ray models of the san Fernando earthquake, Bull. Seismol. Soc. Am., 69, p. 1131-1341.

Helmberger, D. V. (1974). Generalized ray theory for shear dislocation, Bull. Seismol. Soc. Am., 64, p. 45-64.

Howell. B. F., Jr. (1974). Seismic regionalization in North America based on average regional seismic hazard indix, Bull. Seismol. Soc. Am., 64, p. 1509-1528.

Langston, C. A. (1977). The effect of planar dipping structure on source and receiver responses for constant ray parameter, Bull. Seismol. Soc. Am., 67, 1029-1050.

Langston, C. A. and D. E. Blum (1977). The April 29, 1965, Puget Sound earthquake and the crustal and upper mantle structure of Western Washington, Bull. Seismol. Soc. Am., 67, 693-711.

Langston, C. A. and D. V. Helmberger (1975). A procedure for modelling shallow dislocation sources, Geophys. J. R. astr. Soc., 42, p. 117-130.

Milne, W. G. (1967). Earthquake epicenters and strain release in Canada, Canadian Jour. Earth Sci., 4, p. 797-814.

Mullineaux, D. R., M. G. Bonilla, and J. Schlocker, (1967). Relation of building damage to geology in Seattle, Washington, during the April 1965 earthquake, U.S. Geol. Survey Prof. Paper 575-D, p. D183-D191.

Nuttli, O. W. (1952). The western Washington earthquake of April 13, 1949, Bull. Seismol. Soc. Am., 42, 21-28.

Shakal, A. F. and M. N. Toksoz (1980). Amplification and attenuation of site structure: Puget Sound strong motion, [abstract] Earthquake Notes, 50 p. 20.

Tatel, H. E. and M. A. Tuve (1955). Seismic exploration of a continental crust, Geol. Soc. Am. Spec. Paper 62, 35-50.

Trifunac, M. D., F. E. Udwadia, and A. G. Brady (1973). Analysis of errors in digitized strong-motion accelerograms. Bull. Seismol. Soc. Am., 63, 157-187.

Trifunac, M. D. and V. W. Lee (1974). A note on the accuracy of computed ground displacements from strong-motion accelerograms, Bull. Seismol. Soc. Am., 64, 1209-1219.

Wilson, J. R., M. J. Bartholomew, R. J. Carson (1979). Late Quaternary faults and their relationship to tectonism in the Olympic Peninsula, Washington, Geology, 7, p. 235-239.

Zuercher, H. (1975). A study of the crust in Puget Sound using a fixed seismic source, M.S. thesis, University of Washington, Seattle, Wash.

Table 1

Strong Motion Stations and Source Parameters

Site	Location	Δ, km		Azimuth, Degrees		Back Azimuth, Degrees	
		USCGS	ISC	USCGS	ISC	USCGS	ISC
Olympia Highway Test Lab	47.03°, 122.90°W	69	79	234	238	54	58
Seattle Federal Office Building	47.60°N, 122.33°W	23	21	13	352	193	172
Tacoma County-City Building	47.25°N, 122.45°W	18	25	198	225	18	45

April 29, 1965 epicenters

USCGS: 47.4°N 122.4°W

ISC: 47.41°N 122.29°W

Source Orientation : dip = 70°, rake = -75°, strike = 344°

Seismic Moment : 1.4×10^{26} dyne-cm

Table 2

Strong Motion Instrumentation

Site	Component	Instrument	Free Period (sec)	Damping Ratio	Static Magnification
Olympia Highway Test Lab	vertical	SMA	---	---	---
	S 86°W	SMA	---	---	---
	S 04°E	SMA	---	---	---
Seattle Federal Office Building	vertical	SMA	0.084	10	112
	S 32°E	SMA	0.083	10	119
	S 58°W	SMA	0.084	11	127
	S 58°W	CDM	2.45	10	0.8
	N 32°W	CDM	2.51	9	0.8
Tacoma County-City Building	vertical	SMA	0.078	10	114
	E	SMA	0.078	8	118
	S	SMA	0.076	10	120
	E	CDM	3.90	13	1.0
	N	CDM	4.01	10	1.0

SMA - Strong motion accelerometer

CDM - Carder displacement meter

Table 3

TUM station characteristics and teleseismic P data

location: 47.015N 122.9083W

instrumentation:

SPZ Wilson-Lamison Seismometer
T_o = 1.0sec, T_g = 0.95sec,
MAG = 50K at 1sec

SPNS EW Sprengnether, T_o = 1.4sec,
T_g = 1.4sec, MAG = 1800 at 1sec,

Teleseismic Event P Data:

DATE	TIME	LAT(o)	LONG(o)	M	h	LOCATION
12/27/67	9:17:50	21.29S	68.20W	6.3	91	Chile
7/25/68	7:23:02	30.97S	178.13W	6.5	17	Kermadec
10/15/67	8:00:53	11.92N	85.98W	6.2	181	Nicaragua

Table 4

Expected Strong Motion Amplitudes

A. Velocities

	Component	Amplitude Observed (cm/sec)	Amplitude Calculated (cm/sec)
Olympia	Vertical	3.0	5.3
	S86° W	12.7	16.8
	S04° E	8.0	0.2
Tacoma	Vertical	4.8	4.0
	East	9.8	50.4
	South	4.1	18.5
Seattle	Vertical	3.5	1.1
	S32° E	8.2	24.5
	S58° W	12.5	14.7

B. Displacements

	Components	Amplitude Observed (cm)	Amplitude Calculated (cm)
Tacoma	East	-5.2	-16.0
	North	(~0.5)	-5.9
Seattle	S58° W	-7.5	4.7
	N32° W	+4.5	7.8

Figure Captions

Figure 1: Index map of the Puget Sound Area showing the locations of three strong motion sites, Tumwater station (TUM), and epicenters for the 1965 and 1949 earthquakes. Contours show unconsolidated sediment thickness in feet (after Hall and Othberg, 1974).

Figure 2: Corrected acceleration and velocity recorded at the Olympia Highway Test Laboratory for the 1965 earthquake.

Figure 3: Corrected acceleration and velocity recorded at the Seattle Federal Office Building for the 1965 event.

Figure 4: Corrected acceleration and velocity recorded at the Tacoma County-City Building for the 1965 event.

Figure 5: Corrected velocity and displacement from the Carder displacement meter data at Seattle for the 1965 event.

Figure 6: Corrected velocity and displacement from the Carder displacement meter data at Tacoma for the 1965 event.

Figure 7: Teleseismic P waveforms from three earthquakes recorded at Tumwater station. 'BAZ' is the theoretical back azimuth of the ray approach to the station. The arrows indicate several major P to S converted phases.

Figure 8: Crustal models assumed in the wave calculation.

Figure 9: Comparison of responses calculated using generalized ray theory (Cagniard) and the propagator matrix approximation (Haskell) for a 70 km receiver distance and 60 km source depth in model M1.

Figure 10: Smoothed far-field source time function, S(t), obtained by Langston and Blum (1977) for the 1965 event. V(t) is its time derivative.

Figure 11: A suite of synthetic seismogram calculations appropriate for Olympia velocities assuming each crustal model. P_V and P_R are the vertical and radial responses, respectively, due to an incident P wave. SV_V and SV_R are the vertical and radial responses, respectively, due to an incident SV wave.

Figure 12: Synthetic velocities appropriate for Tacoma and Seattle. Same scheme as Figure 11.

Figure 13: Synthetic seismograms assuming several crustal models for Tumwater teleseismic data. A simple pulse-like wave form, similar to the vertical component of the 12/27/67 event of Figure 7 was convolved with each impulse response.

Figure 14: Corrected acceleration and velocity recorded at the Olympia site for the 1949 earthquake.

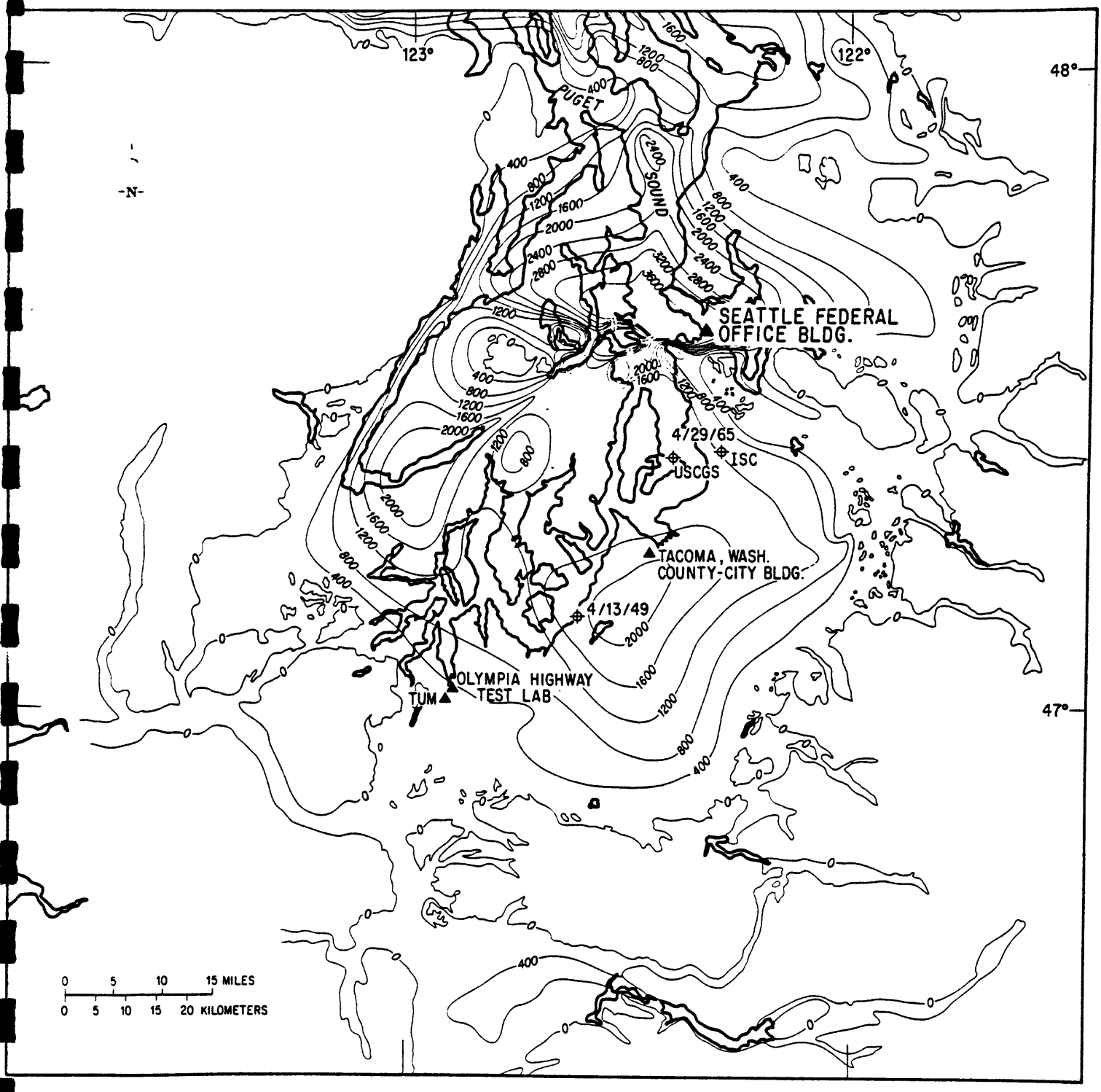
123°
122°
48°
47°
-N-
PUGET SOUND
SEATTLE FEDERAL OFFICE BLDG.
4/29/65
ISC
USCGS
TACOMA, WASH. COUNTY-CITY BLDG.
4/13/49
OLYMPIA HIGHWAY TEST LAB
TUM
0 5 10 15 MILES
0 5 10 15 20 KILOMETERS

Fig. 1

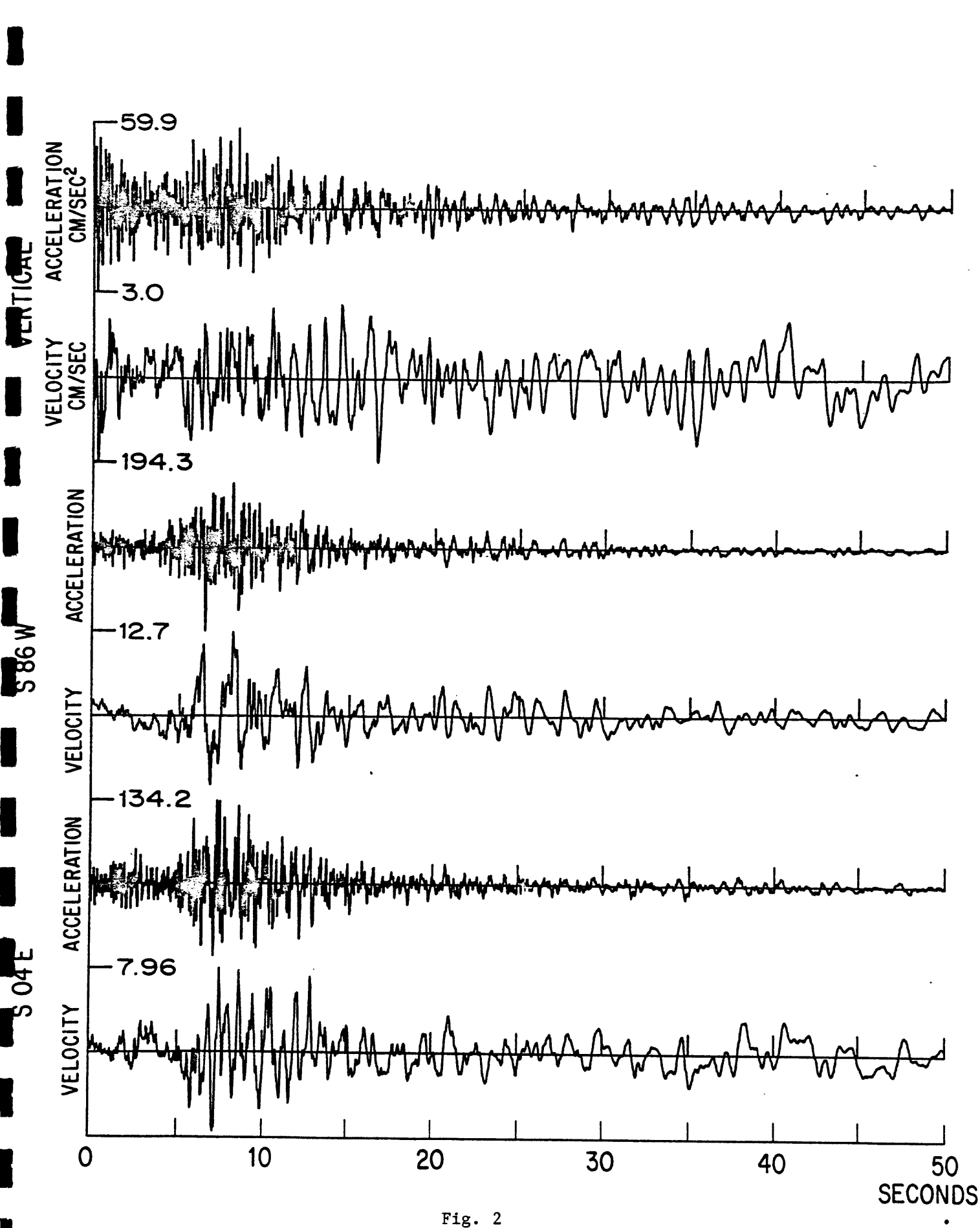
59.9
ACCELERATION CM/SEC²
VERTICAL
3.0
VELOCITY CM/SEC
194.3
ACCELERATION
S86W
12.7
VELOCITY
134.2
ACCELERATION
S04E
7.96
VELOCITY
0
10
20
30
40
50
SECONDS

Fig. 2

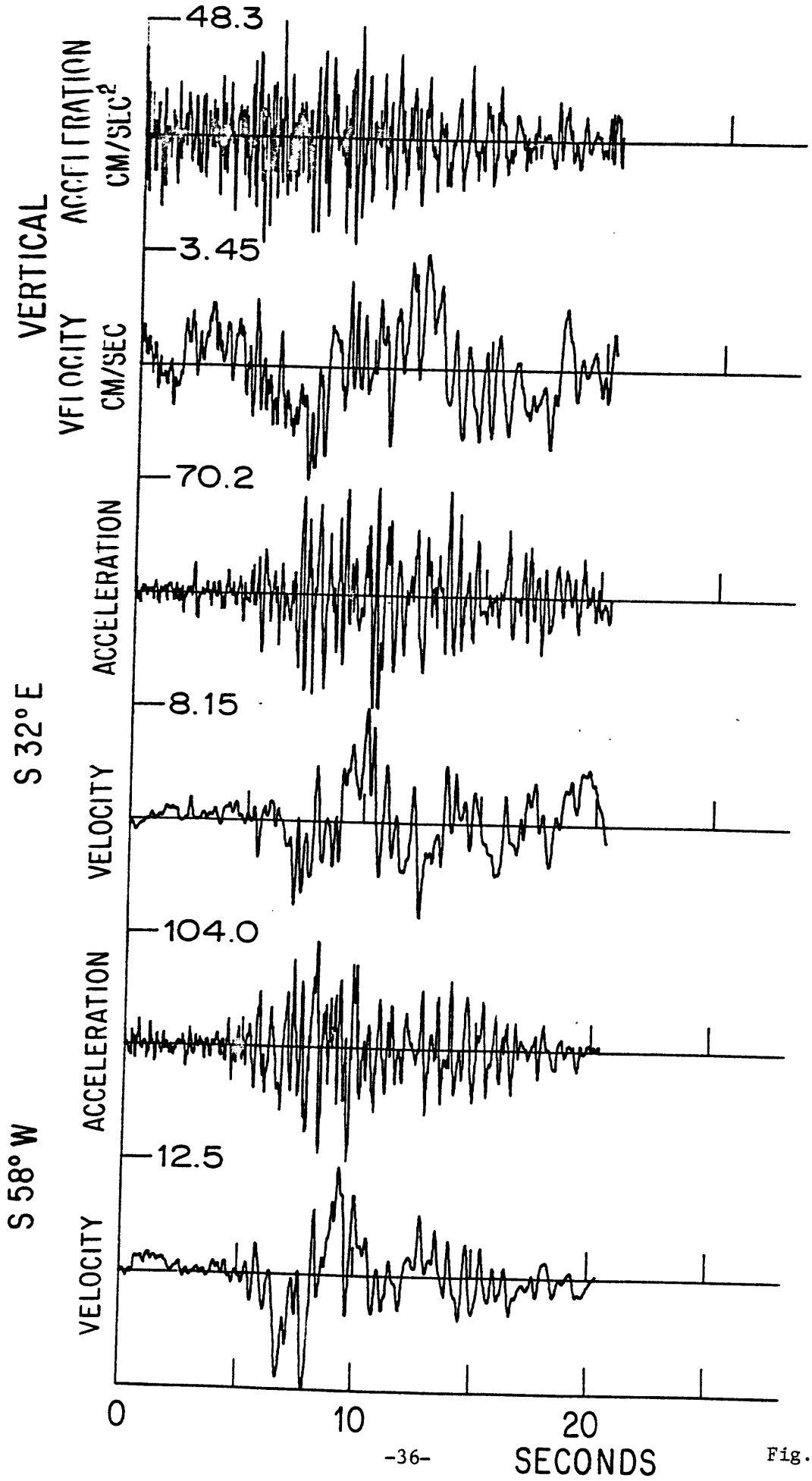
48.3
VERTICAL
ACCELERATION CM/SEC²
3.45
VELOCITY CM/SEC
70.2
S 32° E
ACCELERATION
8.15
VELOCITY
104.0
ACCELERATION
S 58° W
12.5
VELOCITY
0
10
20
SECONDS

Fig. 3

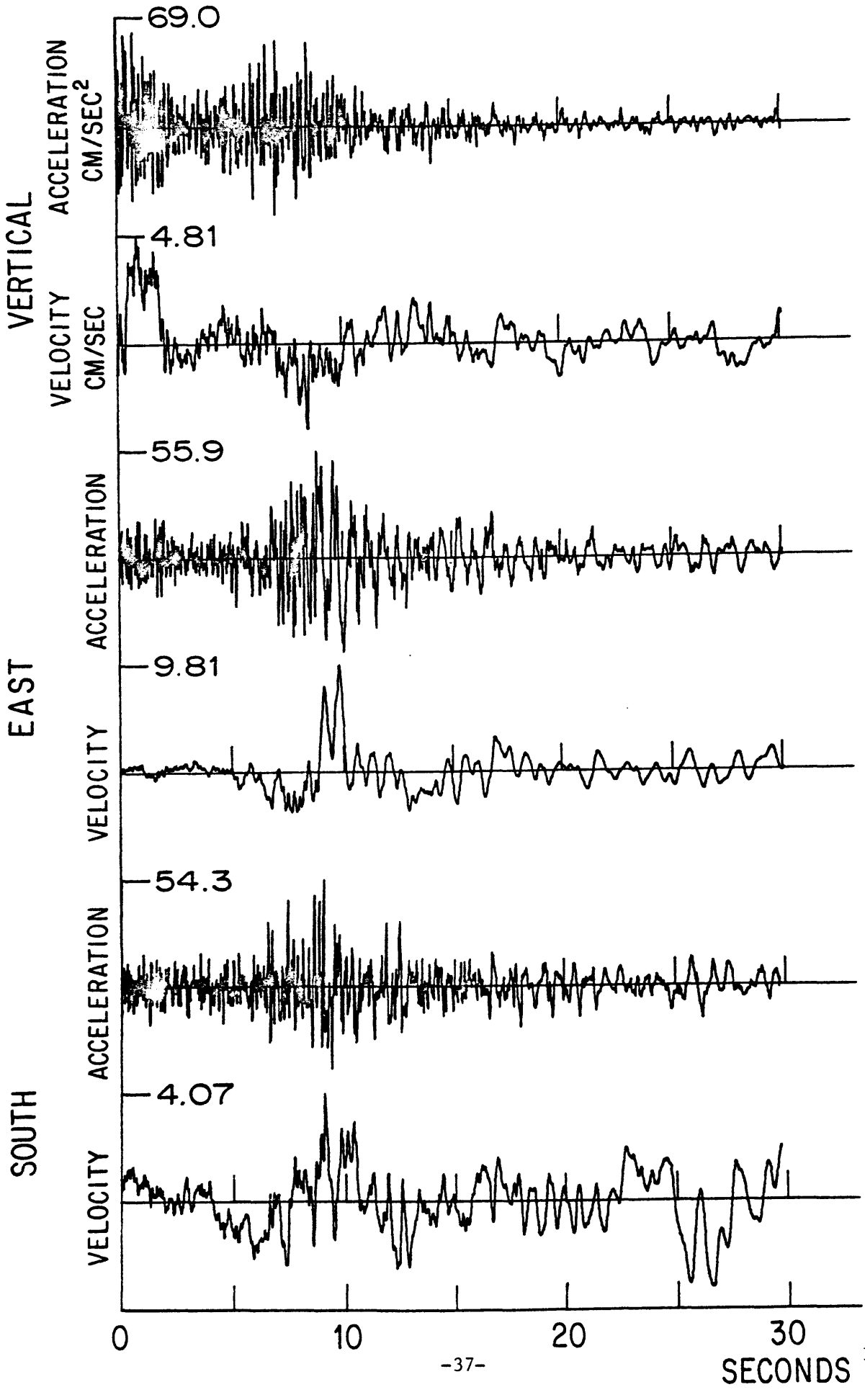
VERTICAL
ACCELERATION CM/SEC²
69.0
VELOCITY CM/SEC
4.81
EAST
ACCELERATION
55.9
VELOCITY
9.81
SOUTH
ACCELERATION
54.3
VELOCITY
4.07
0
10
20
30
SECONDS

Fig. 4

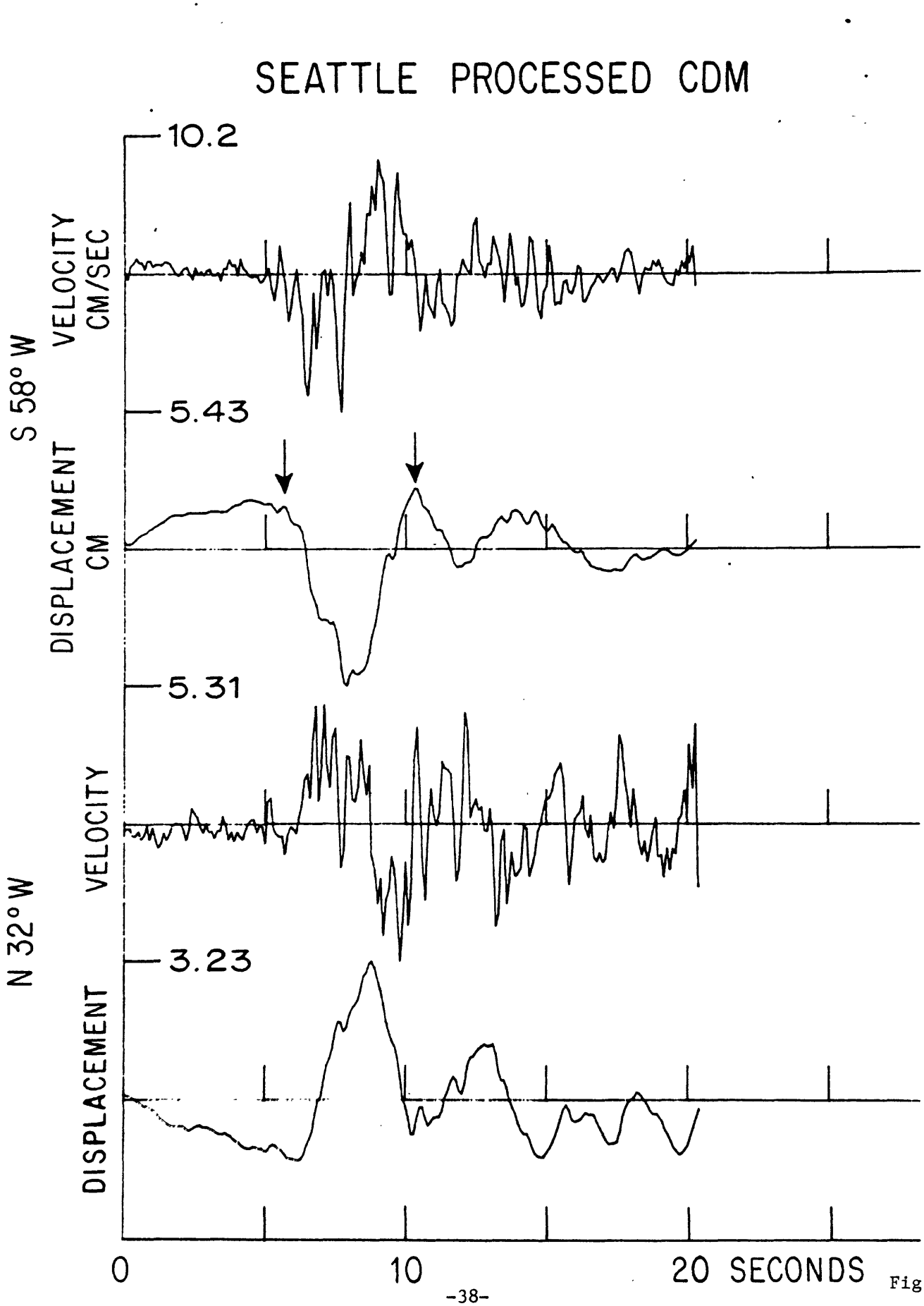
SEATTLE PROCESSED CDM
10.2
S 58° W
VELOCITY
CM/SEC
5.43
DISPLACEMENT
CM
5.31
N 32° W
VELOCITY
3.23
DISPLACEMENT
0
10
20 SECONDS

Fig. 5

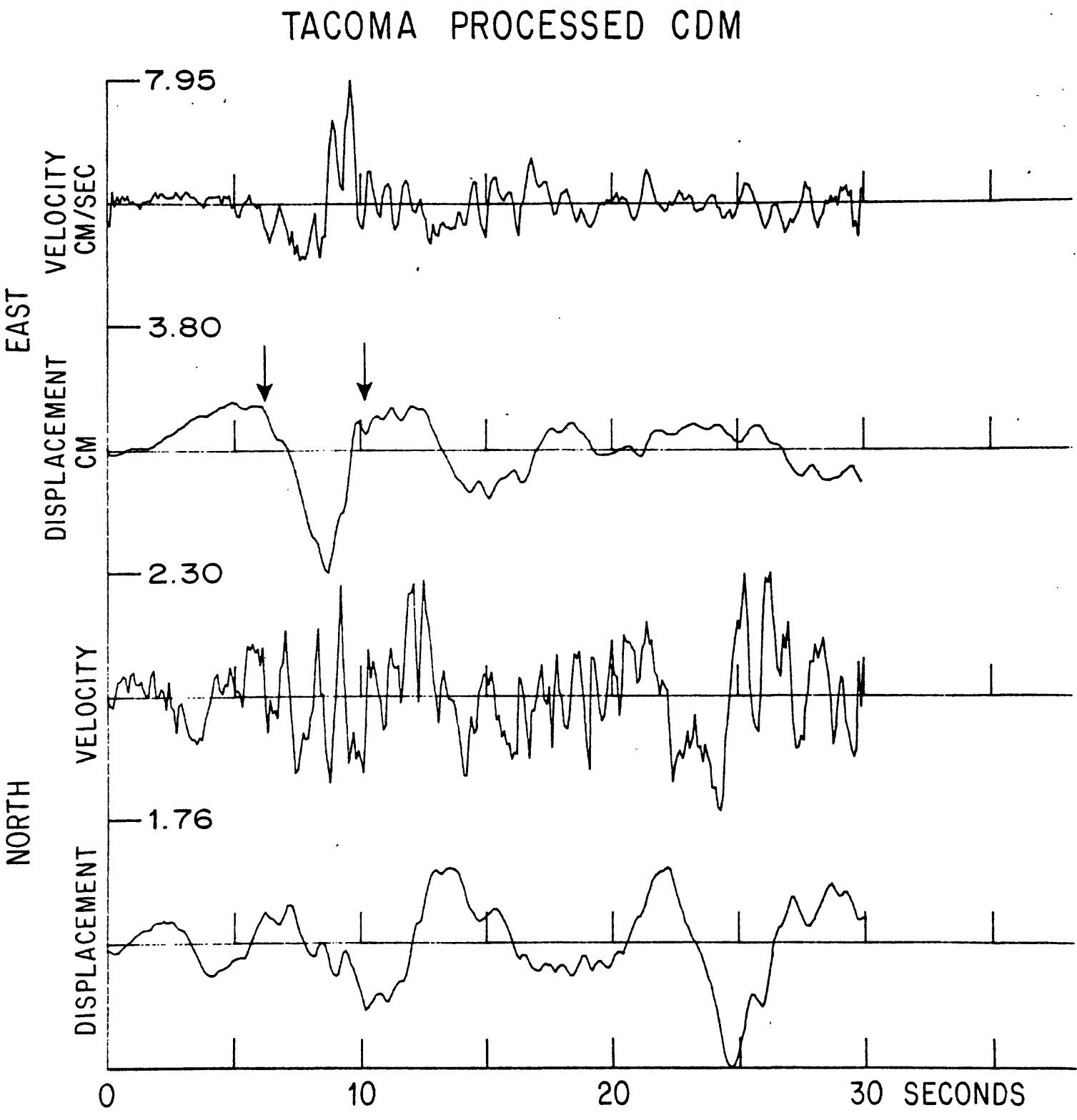
TACOMA PROCESSED CDM
7.95
VELOCITY CM/SEC
EAST
3.80
DISPLACEMENT CM
2.30
VELOCITY
NORTH
1.76
DISPLACEMENT
0
10
20
30 SECONDS

Fig. 6

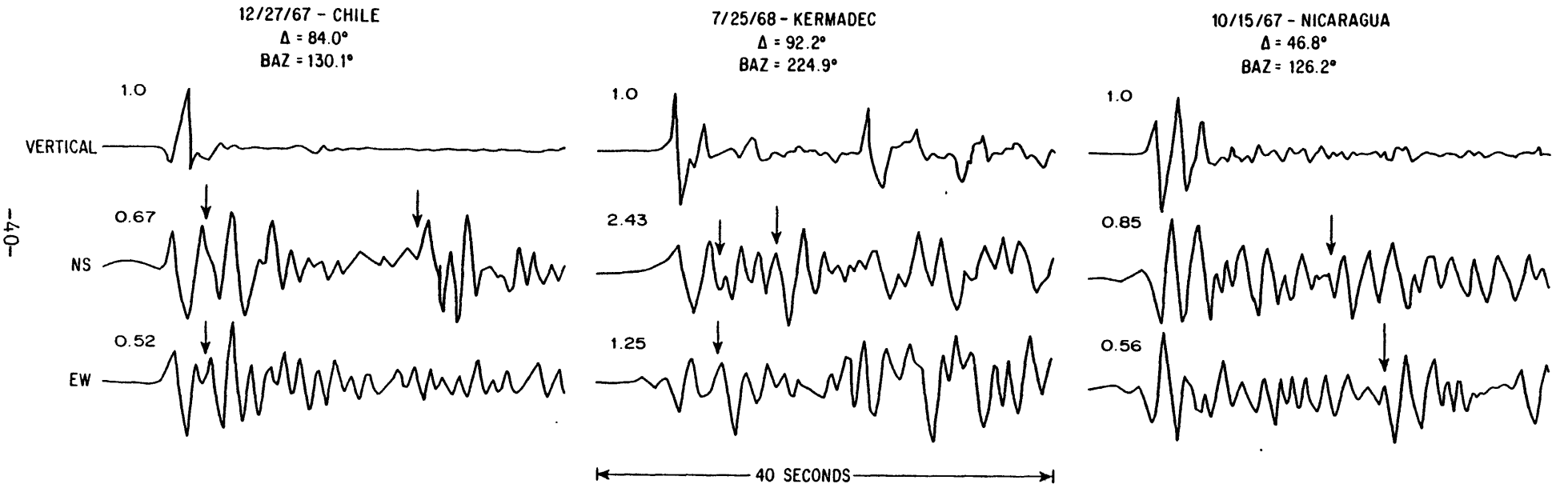
12/27/67 - CHILE
Δ = 84.0°
BAZ = 130.1°
7/25/68 - KERMADEC
Δ = 92.2°
BAZ = 224.9°
10/15/67 - NICARAGUA
Δ = 46.8°
BAZ = 126.2°
1.0
VERTICAL
0.67
NS
0.52
EW
1.0
2.43
1.25
1.0
0.85
0.56
40 SECONDS

Fig. 7

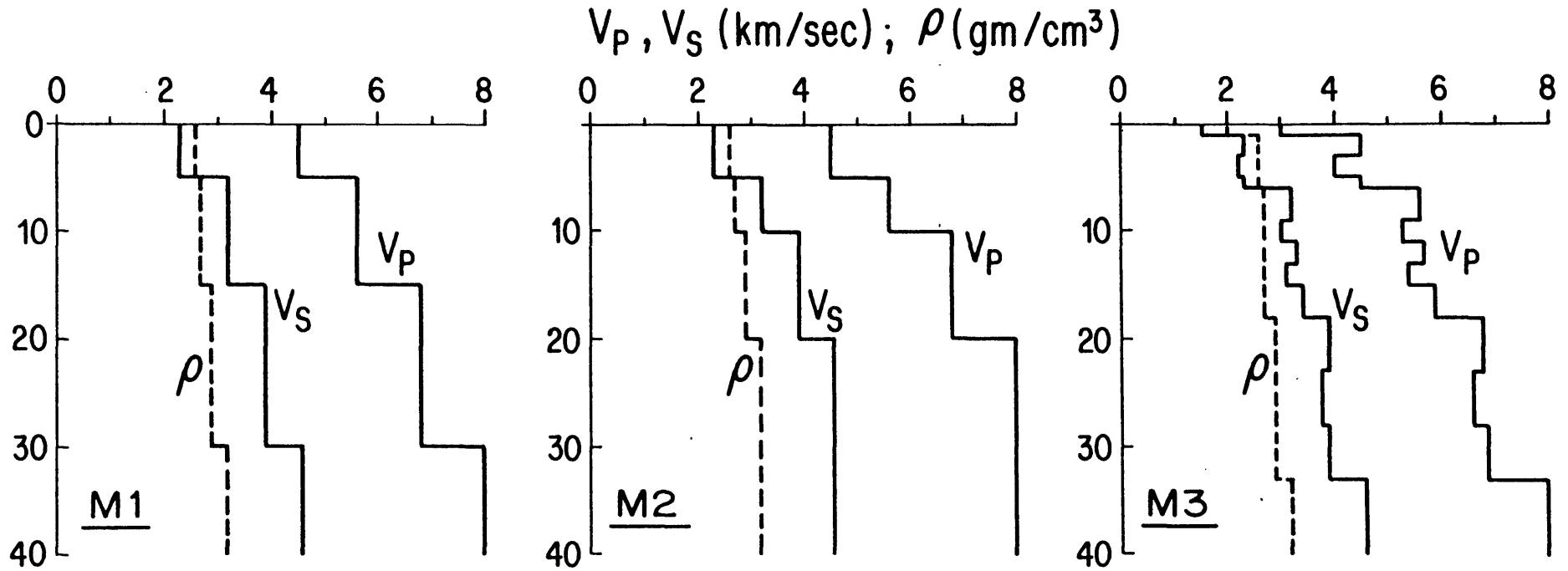

Fig. 8

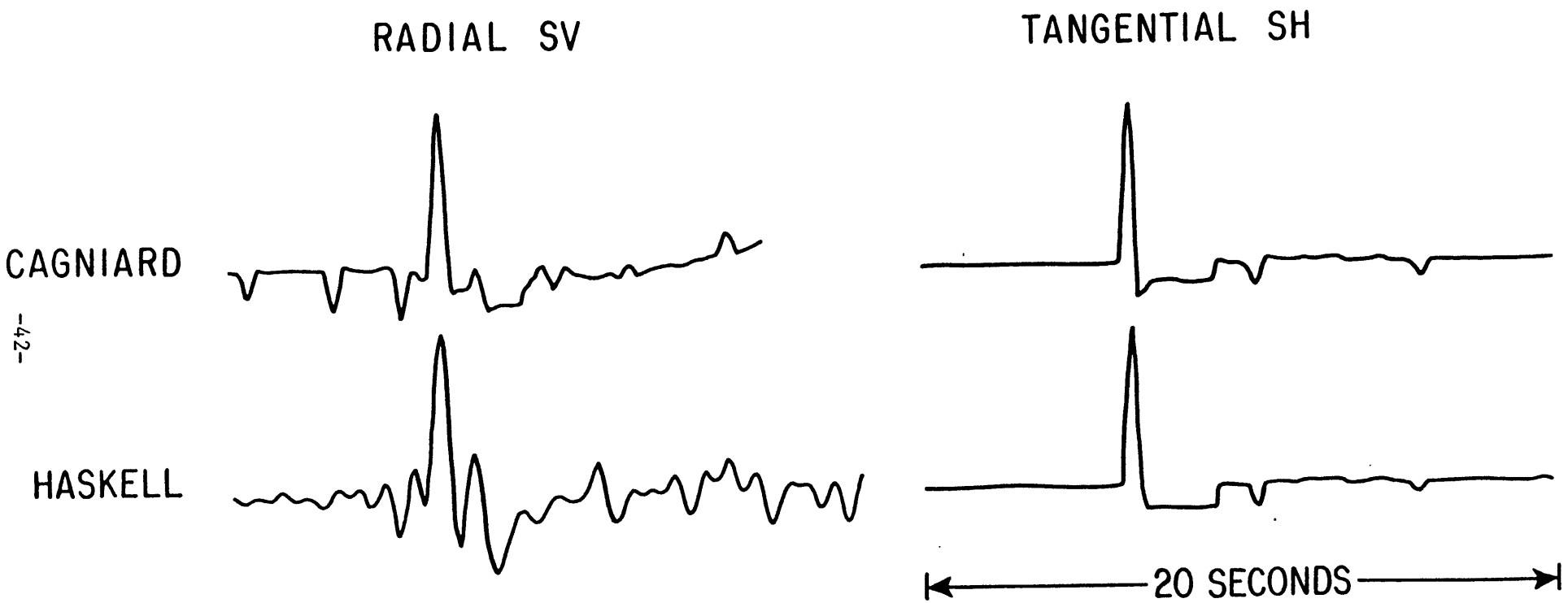

Fig. 9

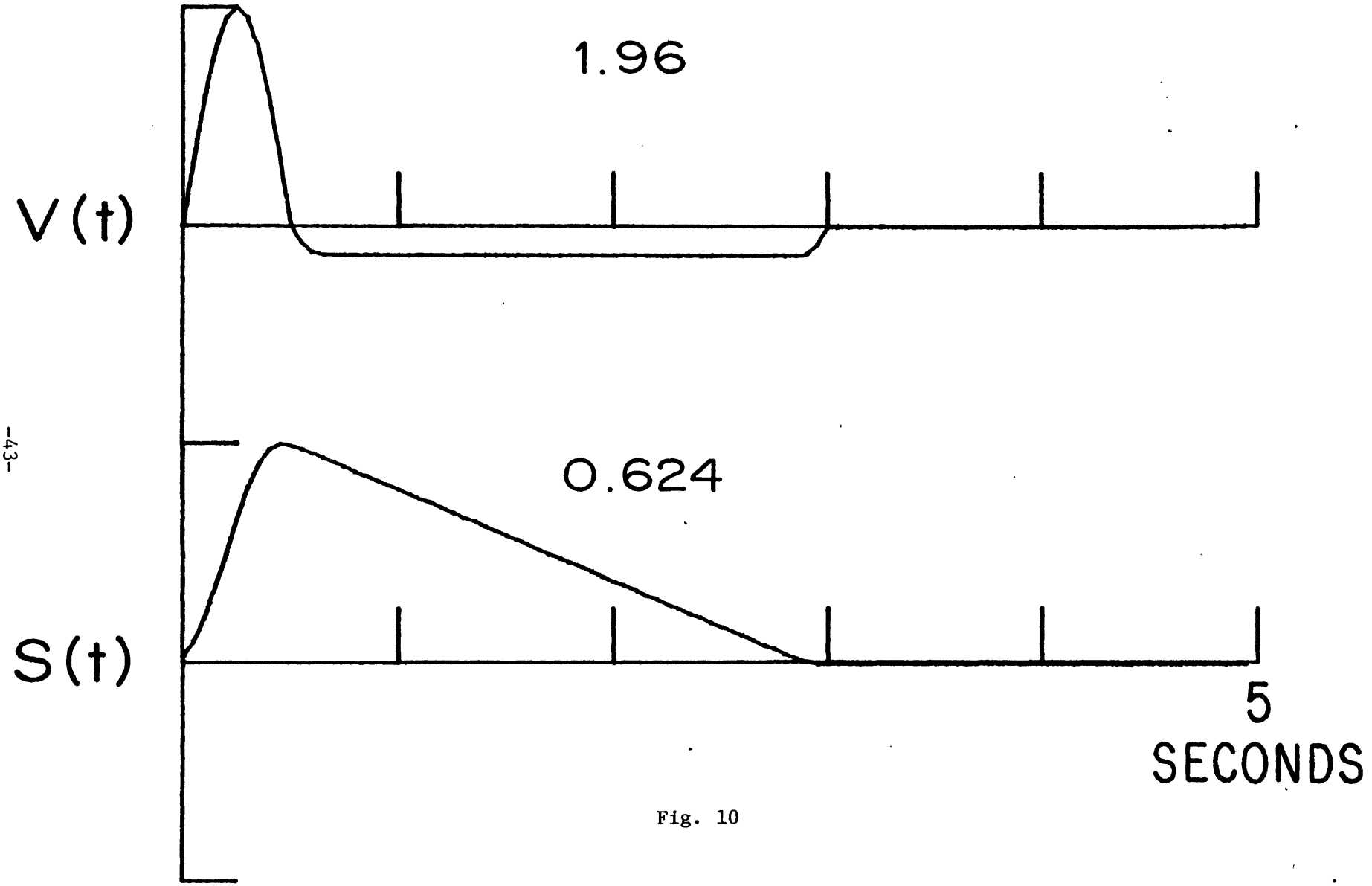

Fig. 10

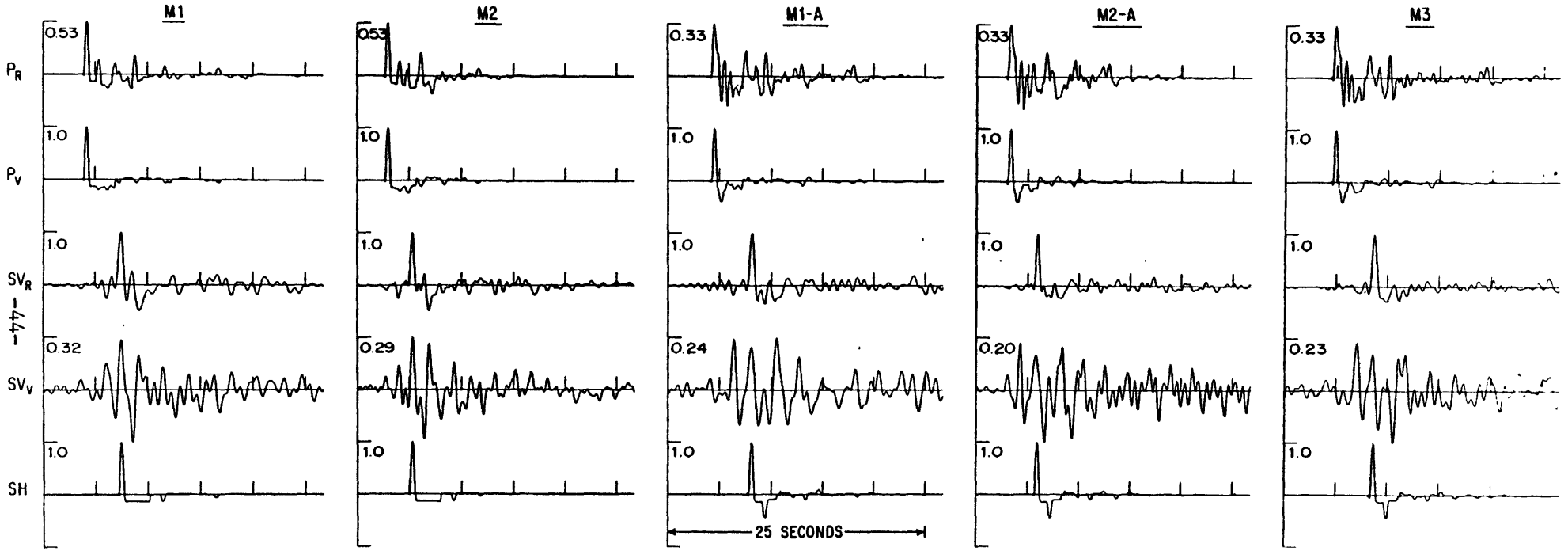
M1
M2
M1-A
M2-A
M3
0.53
0.53
0.33
0.33
0.33
P_R
1.0
1.0
1.0
1.0
1.0
P_V
1.0
1.0
1.0
1.0
1.0
SV_R
0.32
0.29
0.24
0.20
0.23
SV_V
1.0
1.0
1.0
1.0
1.0
SH
25 SECONDS

Fig. 11

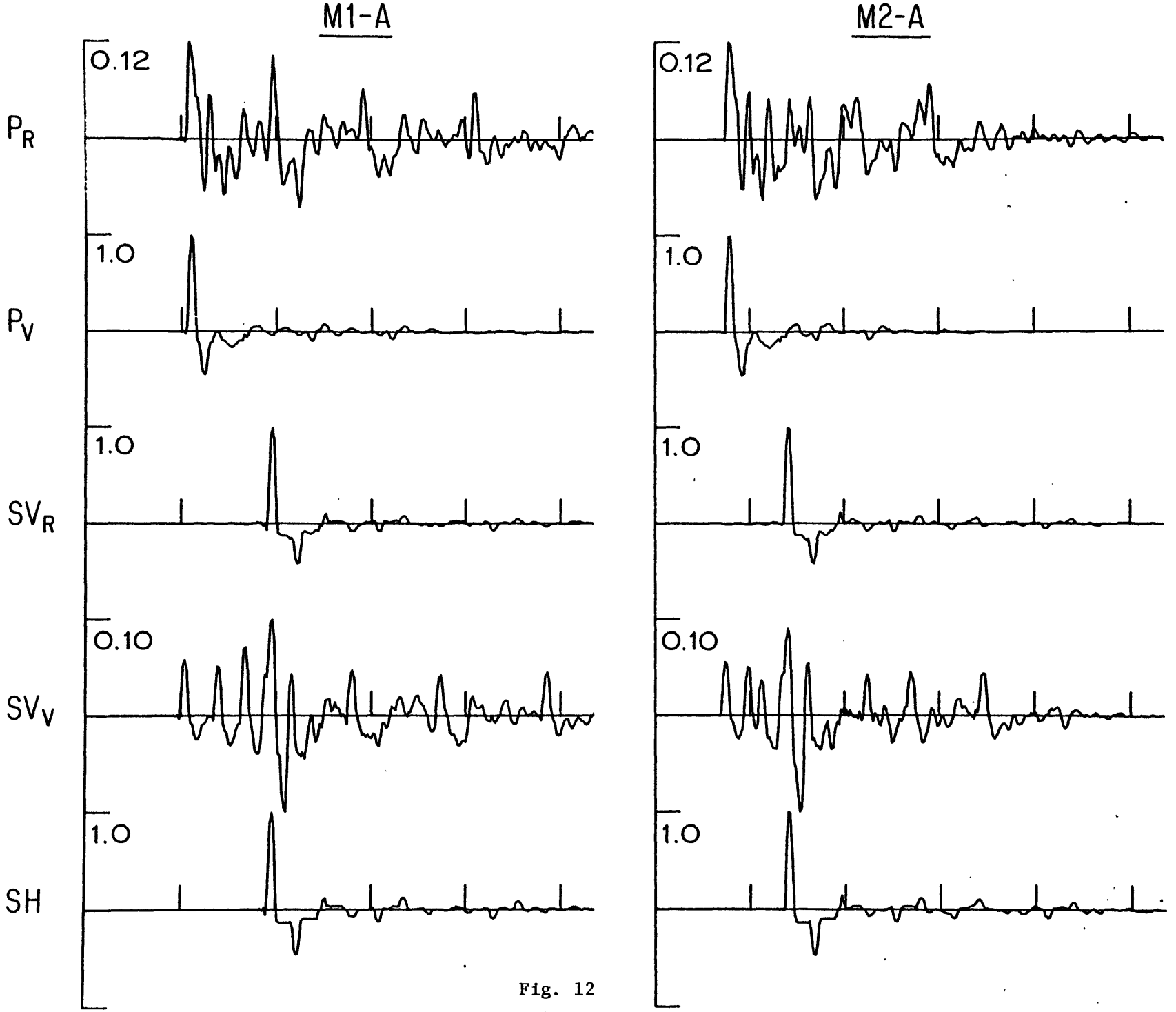

Fig. 12

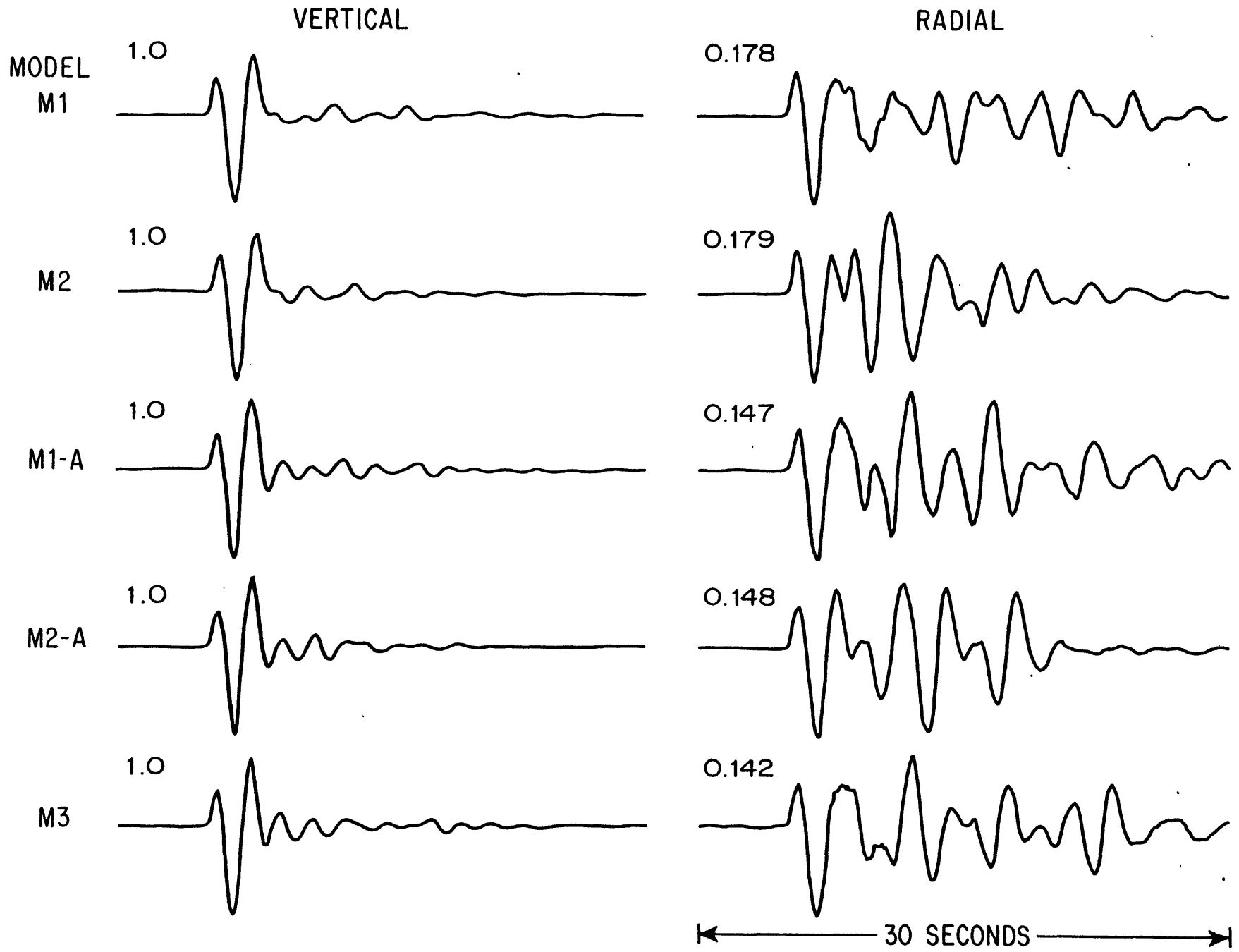
VERTICAL
RADIAL
MODEL
M1
1.0
0.178
M2
1.0
0.179
M1-A
1.0
0.147
M2-A
1.0
0.148
M3
1.0
0.142
30 SECONDS

Fig. 13

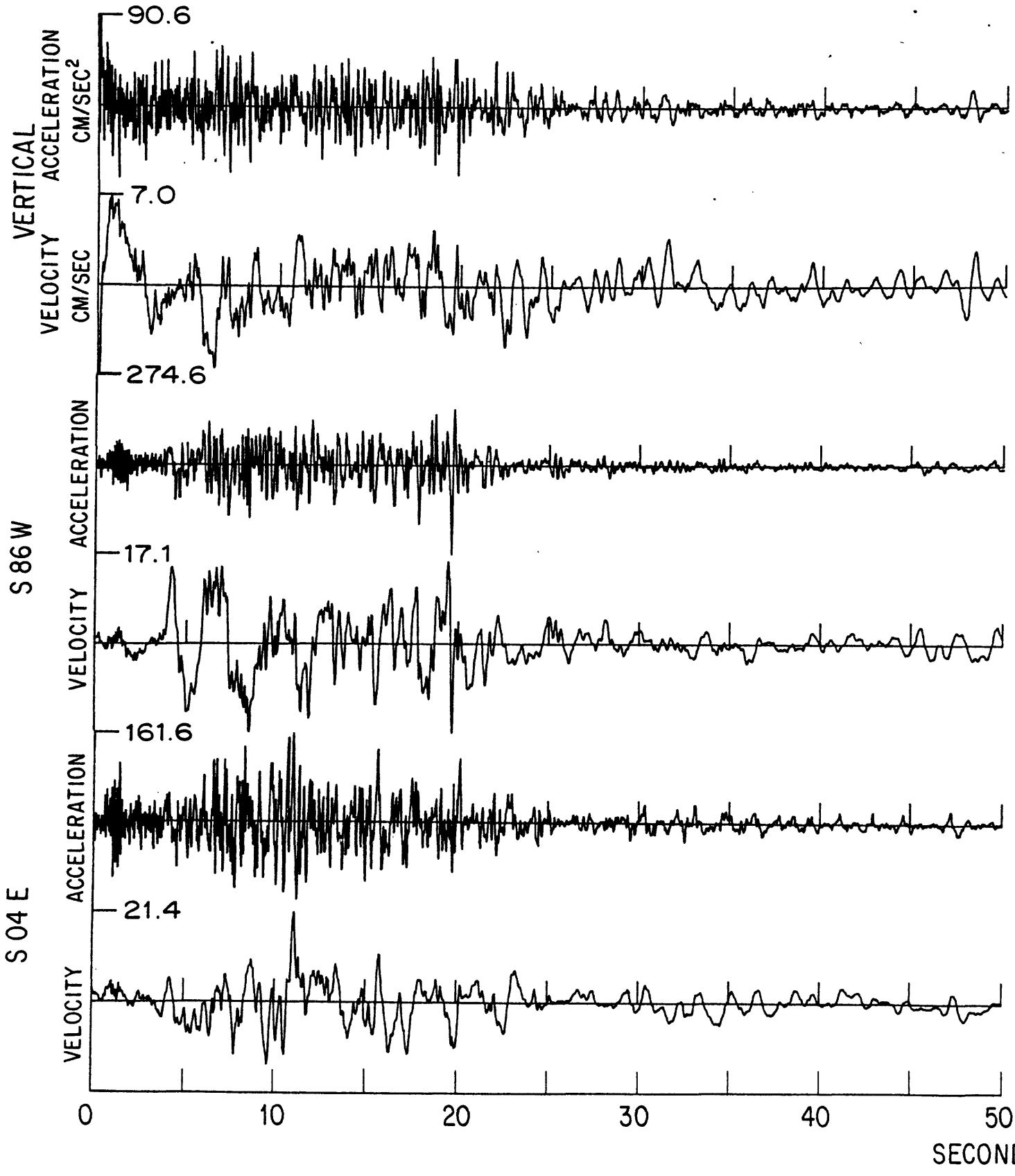
VERTICAL
ACCELERATION CM/SEC²
90.6
VELOCITY CM/SEC
7.0
274.6
S 86 W
ACCELERATION
17.1
VELOCITY
161.6
S 04 E
ACCELERATION
21.4
VELOCITY
0
10
20
30
40
50
SECONDS

Fig. 14

Technical Discussion - Part II:

"Evidence for the Subducting Lithosphere Under Southern Vancouver Island and Western Oregon from Teleseismic P Wave Conversions"

(to be submitted to the Journal of Geophysical Research)

ABSTRACT

Long-period teleseismic P waves recorded at VIC (Victoria, British Columbia) and COR (Corvallis, Oregon) show anomalously large Ps conversions and later arriving P-to-S reverberations not observed from typical continental crustal sections or from previously proposed structures for these stations determined from refraction surveys. The timing and large amplitude of the Ps phase, relative to direct P, suggests a high velocity-contrast interface at 45 to 50 km depth under VIC and COR forming the base of a distinct low velocity zone. This interface is proposed to be the oceanic Moho which is being subducted under North America. Off azimuth Ps recorded at COR is consistent with a 20° eastward dip for the interface. Horizontal particle motion at both sites show evidence for lateral heterogeniety in local crustal structure. The distinct low velocity zone and its negative velocity gradient with depth has important consequences for refraction interpretation in the region. In principle, this type of structure suggests a solution for the Vancouver Island crustal thickness problem.

Introduction

In terms of its size, the Juan de Fuca plate system (Figure 1) is but a minor aspect of global tectonics yet has profound significance towards the unraveling of geologic history and structure in Western United States. The present day interaction of the Juan de Fuca plate with North America also plays no small part in assesments of geologic and geophysical hazards for the Pacific Northwest region. This paper examines a structural aspect of the interaction by presenting direct seismic evidence for the subducting lithosphere under western Oregon and southern Vancouver Island. This evidence consists of teleseismic Ps converted waves from an interface at 45 to 50 km depth under the stations COR (Corvallis, Oregon) and VIC (Victoria, B.C.).

It is ironic, in many respects, that many of the ideas that formed Plate Tectonics in the 1960's were developed from data taken from the Pacific Northwest region. The offshore magnetic anomaly map presented by Raff and Mason (1961) and subsequently interpreted by Wilson (1965), Vine and Wilson (1965), and Vine (1966) represent milestones in the development of global tectonics. Yet many of the normal characteristics attributed to plate movement and subduction for other larger plates in the world are absent or modified for the Juan de Fuca plate. For example, there is no inclined seismic zone under the northwest coast which would be expected on the basis of the offshore magnetic anomalies and presence of andesitic volcanism in the Cascades (Atwater, 1970; Dickinson, 1970; Silver, 1971a; Riddihough, 1978, 1979). Due to high rates of coastal sedimentation there is also no obvious trench where the oceanic crust and lithosphere should plunge under the continent (Silver, 1971b). Further, the Juan de Fuca plate itself goes

against standard tenets of rigid moving plates by exhibiting structures and seismicity which indicate that it is actively being deformed (Tobin and Sykes, 1968; Chandra, 1974; Silver, 1971b; Hyndman et al., 1979). Thus, although it is clear that subduction has occurred in the past in this area, it is not clear that it is continuing. Recent geodetic interpretations for western Washington suggest the unusual possibility that it may be occurring aseismically (Ando and Balazs, 1979).

Aside from trying to define the subduction process for the Juan de Fuca plate more precisely, this work is also motivated by a desire to find ways of directly observing subduction zone structure using seismic means. It is somewhat disconcerting that some of the largest tectonic structures on earth can only be inferred indirectly by seismicity plots or ambiguous earthquake travel time residuals. This problem has been alleviated somewhat for highly active subduction zones. Recent work with the body wave phase conversion ScS-p observed with local networks situated near the source and over the subduction zone has shown good promise in mapping the subducting lithosphere (Sacks and Snoke, 1977; Snoke, et al., 1977). Nevertheless, in areas of little intermediate or deep seismicity, such as the Pacific Northwest, other means must be found. The results of this work suggest that phase conversions from teleseismic P waves recorded at networks or receivers over the subducting zone may be a useful reconnaisance tool in this regard.

Expanding on a study of crustal structure at COR determined from teleseismic body wave techniques (Langston, 1977a), more teleseismic body wave data from COR and VIC have been analyzed in an effort to map the extent and geometry of a distinct high velocity-contrast interface under COR. Because of the high contrast needed to produce large observed P to S conversions

and from absolute velocity control afforded by a local refraction profile (Berg, et al. 1966), it was also inferred that a distinct P and S wave low velocity zone was needed above the interface. Evidence is presented that this structure extends to, or at least is present under, southern Vancouver Island as well. Furthermore, high quality data recorded at COR for the nuclear test Cannikin shows that the high contrast interface dips gently eastward. The interpretation is made that the high contrast interface and low velocity zone above it are the subducting oceanic Moho and crust, respectively. Using this interpretation and results from previous studies, a preliminary cross section of the subducting slab is proposed which shows dips of only 10^{o}-20^{o} until it plunges steeply under the Cascades at about 50^{o} approximately 140 km inland. This type of velocity inversion structure also suggests a solution to the Vancouver Island crustal structure problem (Riddihough, 1979) in which the large crustal thickness of 50 km determined by White and Savage (1965) is incompatible with gravity measurements.

Teleseismic Body Wave Data and Interpretations

Long period recordings from a number of deep earthquakes were collected from the WWSSN station COR (Corvallis, Oregon) and the Canadian Network station VIC (Victoria, British Columbia) (Figure 1). Deep events with simple pulse-like signatures on the vertical component of ground motion are preferable in this kind of study since later arriving P to S conversions can be seen through a direct comparison of the horizontal components with the vertical (Burdick and Langston, 1976). In addition to these deep teleseisms, the nuclear test Cannikin proved to be exceptionally well recorded at COR and fit the criteria of having a simple pulse-like wave form.

Because of its higher frequency nature, compared to the other earthquakes, the Cannikin data furnished additional insight on properties of boundaries under COR. Table 1 contains parameters for events used in this study.

Sixty seconds of the P wave form data were digitized at an unequal increment and interpolated to an even time spacing of 0.25 seconds. The horizontal components of ground motion were then vectorially rotated into the theoretical ray azimuth of arrival to obtain radial and tangential ground motion. Radial displacement is defined as motion on the horizontal plane away from the source and tangential as horizontal motion perpendicular to the radial component and positive clockwise about the source when looking downwards. Figures 2 and 3 show the digitized data for COR and VIC, respectively. Instrument calibration pulses were checked for the COR data to make sure calibration was nominal. However, VIC station was not equipped with calibration circuitry at the times of events listed in Table 1 (Shannon, et al., 1975). Shannon et al. (1975) also indicate that the gain for the long-period NS component was anomalously high during a June 1974 calibration check. Using their values, the amplitude of the NS components for both 1974 events recorded at VIC were decreased appropriately before rotation. Calibration data for other times are not available. However, VIC instrumentation changed from the 30-90 system (1967 events) to the 15-90 system (all later events). Thus, wave form consistency between the data recorded by different instrumentation should indicate the effects of local crustal structure.

A primary reason for decomposing the horizontal ground motion into radial and tangential components is to evaluate the effects of non-horizontally layered structure (Langston, 1977b, 1979). The response of a series of isotropic plane layers to an indicent P plane wave should be contained only in the radial and vertical planes. The presence of dipping interfaces or anisotropy (Keith and Crampin, 1977) will produce tangential ground motion.

In all cases (Figure 2 and 3) tangential motions are obtained after rotation which are often significantly above the seismic noise. Because the tangential component is the weighted difference between the two horizontal components small misalignments of the traces before rotation, instrument miscalibration, and digitizing errors can contribute to spurious high frequency tangential arrivals. These kinds of arrivals can be seen in some rotations as occurring near the times of zero crossings on the radial component. However, if tangential arrivals occur at times where there are clear and obvious differences between the NS and EW components, then these represent true earth structure effects.

In the COR data (Figure 2) most earthquake NS and EW wave forms have easily seen but somewhat small differences. Calculated tangential components are not very consistent between close events, however, so they are assumed to be dominated by processing noise. Data for Cannikin is the exception to this because of the striking but clear difference between arrivals on the NS and EW components. In particular, note the large impulsive arrival on the NS component which is nearly absent on the EW at about 15 seconds. This large secondary arrival clearly rotates into the tangential component.

The tangential waveforms obtained from the VIC data are as problematical as those from the COR earthquake data. In all cases there are obvious differences between NS and EW components indicating non-horizontal structure under southern Vancouver Island. Although there are significant tangential components, overall wave shapes vary considerably between events from similar back azimuths again indicating a predominance of processing noise. This was not a surprising result since it was difficult to find and digitize suitable wave from data from VIC, as compared to COR, due to a combination of higher instrument gain and higher noise levels.

Radial wave forms obtained from both data sets are numerically more stable since they are sums of the horizontals. A comparison of radial components between VIC and COR show many waveform similarities. Note in particular the large oscillations after direct P. These are composed of P to S conversions in the crustal structure beneath the station. Corresponding arrivals do not show up at similar times on the vertical component since the incident angle for teleseismic P waves is relatively steep; converted S waves will be polarized almost entirely in the horizontal plane.

Figure 4 presents a suite of synthetic seismograms for a layer-over-halfspace crust model (Table 2). Because the crust-mantle boundary has a rather severe velocity contrast in this model, large P to S conversions and reverberations are set up within the layer and are seen as a series of arrivals on the radial component. As layer thickness increases the arrival times increase, having the effect of producing a longer duration radial component. Thus, the timing of various phases are related to layer velocity and thickness and the relative amplitude related to interface velocity contrasts.

In a previous study (Langston, 1977a) this information was used to deduce a horizontally plane layered model for COR using the earthquake wave forms of Figure 2. Figure 5 shows that the inferred model is unusual, having a distinct P and S velocity low velocity zone (LVZ) with a high contrast base. The upper 20 kilometers of the model is based on a local refraction profile (Berg et al., 1966) which indicated an 8.0 km/sec refractor at 16 km depth. The large Ps conversions and reverberations required the high contrast interface and LVZ at depths greater than the inferred Moho. Refer to the previous work for details.

To compare the relative effects of structures under COR and VIC we employ a P wave equalization technique discussed by Langston (1979). This technique amounts to deconvolving the vertical component from the radial to remove the effects of instrument and effective source time function. This time series is then convolved with a Gaussian function of approximately four seconds width. The Gaussian filter removes high frequency noise and produces a zero phase pulse at each arrival on the radial seismogram. This method works well in separating P to S conversions from source function and instrument effects because the vertical component of ground motion is composed almost entirely of the direct P wave. See Langston (1979) for details.

Figure 6 represents radial component equalizations for the highest quality earthquake data recorded at COR and VIC. These were chosen on the basis of the signal-to-noise ratio of the data and data processing. For example, the 12-27-67 event at VIC was excluded since the trace line thickness was large compared to signal amplitude masking pulse width and shape details. Although there is some noise in these deconvolutions, as evidenced by the small oscillation before the main P wave on some traces, there is a remarkable consistency in the arrival time and amplitude of the Ps conversion previously interpreted to occur at the base of the COR low velocity zone. This arrival is evident in both COR and VIC data sets. Later arrivals after Ps are less consistent from trace to trace even within the same stations' data set. These arrivals are inferred to be reverberated phases within the crust and upper mantle. Because there are clear indications that non-horizontal structure exists at both stations, it is evident that reverberations will traverse increasingly more distorted ray paths with each reflection or refraction within the structure. This is supported by ray calculations in simple dipping

structures (Langston, 1977b; Hong and Helmberger, 1978). Hence, we may expect a priori that reverberations will be less stable than primary conversions. Synthetic radial component seismograms for the COR model of Figure 5 and the refraction model for Vancouver Island proposed by White and Savage (1965) (also in Table 2) are shown below the data deconvolutions. The major deficiency in the White and Savage model is the lack of high amplitude Ps conversions and reverberations. The observed high amplitudes of these phases at COR and VIC are difficult to reconcile with standard continental crust models without recourse to a high contrast interface at 45 to 50 km depth. The arrival time of the Ps conversion in the White and Savage model does agree well since their crustal column is 50 km thick. However, their crustal thickness determination was based on the negative evidence of not observing a P_n head wave out to several hundred kilometers. From a surface wave dispersion study, Wickens (1977) also suggested that the Moho under Vancouver Island was at 50 km depth. However, the Rayleigh and Love wave data were inconsistent indicating lateral refraction effects or anisotropy. These body wave data, therefore, are the first direct evidence for the Moho under Vancouver Island. This is, of course, dependent on how one defines the Moho given a major velocity inversion.

Returning to structure at Corvallis, some insight on the geometry of the proposed LVZ can be obtained by examining the striking tangential arrivals seen in the Cannikin data. Figure 7 displays the rotated wave form data and a series of synthetic model calculations. By its timing and particle motion, the large secondary arrival on the tangential component corresponds to the inferred Ps conversion from the base of the LVZ. Because the relative amplitude of tangential Ps to tangential P is radically

different than that observed for the same phases on the radial component, most, if not all, tangential motion must be due to dip on the high contrast interface at 45 km depth. To test this assertion synthetic seismograms were calculated assuming the parameters of the COR model and allowing the 45 km depth interface to dip eastward by varying amounts. Details of the ray tracing procedure used to calculate the structure response can be found in Langston (1977b). The vertical component of the Cannikin data was convolved with these impulse responses to obtain the final synthetics. For the same reason given in the equalization method this is a valid procedure since it is exceedingly difficult to produce or observe any arrival of significance on vertical P other than the direct wave. The vertical synthetics of Figure 7 show that this assumption is at least self consistent.

Figure 7 demonstrates that a dip of about 20° reasonably explains the vertical/tangential amplitude ratio and that any eastward dip explains the tangential Ps/P ratio. Westward dip would reverse the tangential component polarity. The major discrepancy between synthetic and observed occurs for the radial component. Apparently, the velocity contrast at the 16 km depth Moho is too strong in the COR model producing an anomalously large Ps conversion. This has little effect on the LVZ Ps conversion so no further modeling was attempted. The apparent large radial amplitude is mainly due to the 16 km Ps phase; note that first peak amplitudes between data and synthetic are comparable (0.29 versus 0.31, respectively). In this type of modeling it is relatively easy to remove or reduce arrivals by smoothing interfaces with gradient zones in velocity. Also, strike direction is not precisely defined by the amplitude and polarity of only one phase. Thus, the north-south strike assumed in the model calculations is only a best estimate based on the linearity of the Oregon coast and other geologic features.

Discussion

These body wave data indicate that structures under VIC and COR are similar in their gross properties in that a high contrast interface at 45 to 50 km depth is required to produce the large Ps conversion and associated reverberations. Because the depth of this interface is rather unusual to be the Moho for many continental margin structure models and because there is a strong evidence of subduction along the coast, we propose that this major interface represents the Moho of the subducting Juan de Fuca plate. Figure 8 is a cross section of proposed structure perpendicular to the Oregon coast near COR. Offshore structures at G11 and G10 were taken from Shor et al. (1968). By connecting the base of the COR LVZ to the Moho depths obtained from offshore refraction profiling, a relatively gentle dip of about 10^{o} is obtained. The 20^{o} dip inferred from tangential Ps amplitude reasonably agrees with this straight line interpretation.

Three rather ill defined depth zones are indicated for structure near COR in Figure 8 in an attempt to emphasize the dynamic interaction of 'continental' and oceanic structure for subduction along the Oregon-Washington coast. At the top of COR structure is a 16 km thick crustal section with, perhaps, 5 to 10 km of upper mantle material beneath it. This unit probably represents early Tertiary oceanic crust and upper mantle which was emplaced along the west coast of North America when subduction jumped westward from its late Mesozoic-early Tertiary position to its present position 36 m.y. ago (McWilliams, 1978).
This thickened oceanic structure derived by Berg et al. (1966) and Tatel and Tuve (1955) for COR and the Coast Ranges has been used as evidence for this kind of accretionary model for the Columbia Embayment for some

years (Hamilton and Myer, 1966; Muller, 1977; Simpson and Cox, 1977; McWilliams, 1978; Wilson and Cox, 1980). The inferred LVZ is postulated to contain melange-like material, pervasively sheared near the top and grading downwards to largely undeformed subducting oceanic crust. The higher 'mixing zone' may contain an assortment of rock types including some trench sediment, oceanic crust, and previous oceanic upper mantle.

Figure 9 displays a preliminary sketch of the morphology of the subducting oceanic Moho under the Pacific Northwest. In this figure 'distance' is measured perpendicular to the coastline to the respective seismic station or event. The coastline was chosen as a reference since it very nearly follows the trend of the postulated curving trench and because the gravity anomaly signature also parallels the coast (Riddihough, 1979). On Figure 9 depth to the oceanic Moho is plotted from the results of this study and from similar results obtained from the 1965 Puget Sound earthquake (Langston and Blum, 1977). Interpretive fault planes with slip directions are given for the 1965 and the 1949 Puget Sound earthquakes (Hodgson and Storey, 1954; Langston and Blum, 1977). These events had substantial magnitudes of 6.5 and 7.1, respectively and are probably intimately related to subduction processes. The depth under the coastline is taken from Figure 8 and the 100 km depth(?) under LON (Longmire, Washington) is inferred from the presence of Cascade andesitic volcanism and geochemical correlations with depth to Benioff zone in other regions of the world (Dickenson, 1970). Thus, this rough picture indicates that the subducting slab dips at a shallow angle to about 140 to 150 km inland, then plummets under the Cascades with a dip of about 50°. The fault mechanisms are consistent with down-dip extension, similar to mechanisms

in shallow Benioff zones elsewhere (Isacks and Molnar, 1971). The 50° dip is also consistent with structure interpretations made from teleseismic P residuals (McKenzie and Julian, 1971; Lin, 1974).

Crustal structure was purposely ignored in Figure 9 since there are large changes in tectonic style, geology, and structure in the Pacific Northwest region. In particular, the shallow crustal Moho depth near COR of 16 km abruptly deepens to 30 km or more in the Puget Sound depression (Zuercher, 1975). Further, White and Savage (1965) suggested a 50 km crustal thickness for Vancouver Island. This particular thickness determination has presented major problems to geophysical and geological interpretation of Vancouver Island particularly in relation to gravity studies.

Riddihough (1979) thoroughly discusses these problems and presents a possible solution. The major difficulty with a 50 km crustal thickness is that it should produce a large negative Bouguer gravity anomaly. This is not observed, however. In fact, the gravity anomaly is slightly positive and similar to the anomaly observed for coastal Oregon and Washington. Thus, there is no evidence for major changes in structure along the coast except possibly in the Olympic Penninsula. Riddihough (1979) tries to incorporate the results of White and Savage by appealing to high density, low velocity material between 20 and 100 km depth. A slightly more complicated solution is proposed from the similarity of VIC and COR Ps conversions. From the similarity of seismic responses at the two stations and from their similar gravity anomalies, it is suggested that structure under the two sites is not significantly different. The low velocity zone and high velocity, high density cap under COR also extends to VIC or, at least, occurs at VIC. The high density remnant of upper mantle material at the top of the LVZ would help explain the problem with the gravity anomalies

and the negative velocity gradients within this structure could explain the unusual crustal thickness inferred by White and Savage. Negative velocity gradients are difficult to observe with refraction techniques since they are manifest by shadow zones or large apparent attenuation (Hill, 1971). It is likely, therefore, that White and Savage (1965) did not observe P_n because of negative gradients. To demonstrate these effects a synthetic refraction profile was computed for the earth model in Figure 10. The impulse response was computed using the method of generalized rays (e.g., Helmberger, 1968) and convolved with a 0.5 second duration wavelet. Arrival 'A' in Figure 11 is representative of the wavelet shape. The model of Figure 10 was chosen to combine the upper crust velocities found by White and Savage (1965) with a low velocity zone model similar to COR structure. Note the small Moho head wave arrival compared to the large post-critical reflection off the top of the low velocity zone (arrival B). The Moho in this case is defined as the interface at 20 km depth. In the presence of noise or low shot strength, this low amplitude arrival could be masked. Thus, a reevaluation of the data taken by White and Savage (1965) is suggested with special emphasis on probable negative velocity gradients. Other regional refraction profiles should also be carefully interpreted in light of this type of structure.

CONCLUSIONS

The analysis of unusually large Ps conversions and reverberations from teleseisms recorded at Corvallis, Oregon, and Victoria, British Columbia, suggest a high velocity contrast interface at about 45 km depth. This interface forms the base of a distinct low velocity zone and is proposed to be the Moho of subducting oceanic crust of the Juan de Fuca plate. Tangential Ps and P observed at COR for the Cannikin event is consistent with an eastward dip of 20° for the subducting crust. A proposed cross section for the geometry of the subducting Moho shows shallow dips of 10° to 20° to a distance of about 140 km from the coast. The slab then plunges under the Cascades at a dip of about 50°.

The widespread existence of this major low velocity zone structure near the northwest coast of North America also has important implications for interpretations of refraction profiles and travel time studies. In particular, a resolution of the Vancouver Island crustal thickness problem can be, in principle, obtained by considering the effects of negative velocity gradients on previous refraction results. Although unproven here, the 50 km crustal thickness obtained by White and Savage (1965) may be an artifact of misinterpreting refraction shadow zones.

Finally, low velocity zones originating from subducting oceanic crust may be a common feature in every subduction zone and should be incorporated in structure interpretations. They are undoubtably important in causing biases in local earthquake location.

Acknowledgments

I would like to thank Larry Cathles for several suggestions which improved the manuscript. This research was supported by the U.S. Department of the Interior, Geological Survey, under contract No. 14-08-0001-18235.

Table 1

Event Parameters

Date	Time,UT	Position	m_b	H,km	Location
11/03/65	1:39:03.2	9.10S, 71.40W	5.9	583	Peru-Brazil
2/15/67	16:11:11.8	9.05S, 71.34W	6.1	598	Peru-Brazil
9/09/67	10:06:44.5	27.62S, 63.15W	5.9	577	Argentina
12/27/67	9:17:50.3	21.29S, 68.20W	6.3	91	N. Chile
1/19/69	7:02:07.9	44.89N,143.21E	6.3	238	Hokkaido, Japan
11/06/71	22:00:00.1	51.47N,179.11E	7.0	1.8	Aleutians (Cannikin Nuclear Test)
1/05/74	8:33:50.7	12.3 S, 76.4 W	6.3	98	Peru
3/23/74	14:28:35.4	23.9 S,179.8 E	6.1	535	Fiji Islands

Table 2

Structure Models

one-layer over half-space

layer No.	Vp(km/sec)	V_S(km/sec)	ρ(gm/cc)	Th(km)
1	6.0	3.5	2.6	--
2	8.1	4.7	3.2	--

Vancouver Island model (White and Savage, 1965)

1	6.0	3.5*	2.7*	6.2
2	6.73	3.9	2.8	45.0
3	7.74	4.5	3.1	--

*Assigned S velocities and densities not in original study

REFERENCES

Ando, M. and E. I. Balazs (1979). Geodetic evidence for aseismic subduction of the Juan de Fuca plate, J. Geophys. Res. 84, 3023-3028.

Atwater, T. (1970). Implications of plate tectonics for the Cenozoic tectonic evolution of Western North America, Bull. Geol. Soc. Am., 81, 3513-3536.

Berg, J. W., Jr., L. Trembly, D. A. Emilia, J. R. Hutt, J. M. King, L. T. Long, W. R. McKnight, S. K. Sarmah, R. Souders, J. V. Thiruvathukal, D. A. Vossler (1966). Crustal refraction profile Oregon coast range, Bull. Seismol. Soc. Am., 56, 1357-1362.

Burdick, L. J. and C. A. Langston (1976). Modeling crustal structure through the use of converted phases in teleseismic body waveforms, Bull. Seismol. Soc. Am., 67, 677-691.

Chandra, U. (1974). Seismicity, earthquake mechanisms, and tectonics along the western coast of North America, from 42°N to 61°N, Bull. Seismol. Soc. Am., 64, 1529-1549.

Dickinson, W. R. (1970). Relations of andesites, granites, and derivative sandstones to arc-trench tectonics, Rev. Geophys. Space Phys., 8, 813-860.

Hamilton, W. and W. B. Myers (1966). Cenozoic tectonics of the Western United States, Rev. Geophys. Space Phys., 4, 509-549.

Haskell, N. A. (1962). Crustal reflection of plane P and SV waves, J. Geophys. Res., 67, 4751-4767.

Helmberger, D. V. (1968). The crust-mantle transition in the Bering Sea, Bull. Seismol. Soc. Am., 58, 179-214.

Hill, D. P. (1971). Velocity gradients in the continental crust from headwave amplitudes, AGU Monograph 14, 71-75.

Hodgson, J. H. and R. S. Storey (1954). Direction of faulting in some larger earthquakes of 1949, Bull. Seismol. Soc. Am., 44, 57-83.

Hong, Tai-Lin and D. V. Helmberger (1978). Glorified optics and wave propagation in nonplanar structure, Bull. Seismol. Soc. Am., 68, p. 1313-1330.

Hyndman, R. D., R. P. Riddihough, and R. Herzer (1979). The Nootka Fault Zone-a new plate boundary off western Canada, Geophys. J.R. Astr. Soc., 58, 667-683.

Isacks, B. and P. Molnar (1971). Distribution of stresses in the descending lithosphere from a global survey of focal-mechanism solutions of mantle earthquakes, Rev. Geophys. Space Phys., 9, 103-174.

Keith, C. M. and S. Crampin (1977). Seismic body waves in anisotropic media: Synthetic seismograms, Geophys. J. R. Astr. Soc., 49, 225-243.

Langston, C. A. (1977a). Corvallis, Oregon, crustal and upper mantle receiver structure from teleseismic P and S waves, Bull. Seismol. Soc. Am., 67, 713-724.

Langston, C. A. (1977b). The effect of planar dipping structure on source and receiver responses for constant ray parameter, Bull. Seismol. Soc. Am., 67, 1029-1050.

Langston, C. A. (1979). Structure under Mount Rainier, Washington, inferred from teleseismic body waves, Jour. Geophys. Res., 84, 4749-4762.

Langston, C. A. and D. E. Blum (1977). The April 29, 1965, Puget Sound earthquake and the crustal and upper mantle structure of western Washington, Bull. Seismol. Soc. Am., 67, 693-711.

Lin, J. W. (1974). A study of upper mantle structure in the Pacific Northwest using P waves from telseisms, Ph.D. Thesis, University of Washington, Seattle, Wash.

McKenzie, D. and B. Julian (1971). Puget Sound, Washington, earthquake and the mantle structure beneath the northwestern United States, Geol. Soc. Am. Bull., 82, 3519-3524.

McWilliams, R. G. (1978). Early Tertiary rifting in western Oregon-Washington, Am. Assoc. Pet. Geol. Bull., 62, 1193-1197.

Muller, J. E. (1977). Evolution of the Pacific margin, Vancouver Island, and adjacent regions, Can. J. Earth Sci., 14, 2062-2085.

Raff, A. D. and R. G. Mason (1961). Magnetic survey off the west coast of North America, 40°N latitude to 52°N latitude, Bull. Geol. Soc. Am., 72, 1267-1270.

Riddihough, R. P. (1978). The Juan de Fuca plate, EOS, 59, 836-842.

Riddihough, R. P. (1979). Gravity and structure of an active margin-British Columbia and Washington, Can. J. Earth. Sci., 16, 350-363.

Sacks, I. S. and J. A. Snoke (1977). The use of converted phases to infer the depth of the lithosphere-asthenosphere boundary beneath South America, J. Geophys. Res., 82, 2011-2017.

Shannon, W. E., F. Lombardo, B. Compton, and R. J. Halliday (1975). Canadian Seismograph Operations-1974, Seismological Series Number 70, Energy, Mines and Resources Canada, Earth Physics Branch, Ottawa, Canada.

Shor, G. G., P. Dehlinger, H. K. Kirk, and W. S. French (1968). Seismic refraction studies off Oregon and Northern California, J. Geophys. Res., 73, 2175-2194.

Silver, E. A. (1971a). Transitional tectonics and late Cenozoic structure of the continental margin off northernmost California, Bull. Geol. Soc. Am., 82, 1-22.

Silver, E. A. (1971b). Small plate tectonics in the Northeastern Pacific, Geol. Soc. Am. Bull., 82, 3491-3496.

Simpson, R. W. and A. Cox (1977). Paleomagnetic evidence for tectonic rotation of the Oregon Coast Range, Geology, 5, 585-589.

Snoke, J. A., I. S. Sacks, and H. Okada (1977). Determination of the subducting lithosphere boundary by use of converted phases, Bull. Seismol. Soc. Am., 67, 1051-1060.

Tatel, H. E. and M. A. Tuve (1955). Seismic exploration of a continental crust, Geol. Soc. Am. Spec. Paper 62, 35-50.

Tobin, D. G. and L. R. Sykes (1968). Seismicity and tectonics of the northeast Pacity Ocean, J. Geophys. Res., 73, 3821-3845.

Vine, F. J. (1966). Spreading of the ocean floor: New evidence, Science, 154, 1405-1414.

Vine, F. J. and J. T. Wilson (1965). Magnetic anomalies over a young oceanic ridge off Vancouver Island, Science, 150, 485-489.

White, W. R. H. and J. C. Savage (1965). A seismic refraction and gravity study of the earth's crust in British Columbia, Bull. Seismol. Soc. Am., 55, 463-486.

Wickens, A. J. (1977). The upper mantle of southern British Columbia, Can. J. Earth Sci., 14, 1100-1115.

Wilson, J. T. (1965). Transform faults, oceanic ridges and magnetic anomalies southwest of Vancouver Island, Science, 150, 482-485.

Wilson, D. and A. Cox (1980). Paleomagnetic evidence for tectonic rotation of Jurasic plutons in Blue Mountains, Eastern Oregon, Jour. Geophys. Res., 85, 3681-3689.

Zuercher, H. (1975). A study of the crust in Puget Sound using a fixed seismic source, M.S. Thesis, University of Washington, Seattle, Wash.

Figure Captions

Figure 1: Sketch map of the Pacific Northwest region with plate tectonic elements after Riddihough (1978). The track just offshore represents the presumed trench position. Triangles give the position of seismic stations mentioned in this study. The location of the April 29, 1965, Puget Sound earthquake is also indicated.

Figure 2: Teleseismic P waveforms recorded at COR. The date of each event, ray approach back azimuth in degrees (BAZ), and distance in degrees (DEL) are given at the top of each waveform set. Amplitude of the maximum of each trace, relative to the vertical component, is given to the right of each waveform. RAD and TANG are the radial and tangential components of ground motion, respectively.

Figure 3: Teleseismic P wave forms recorded at VIC. Same scheme as Figure 2.

Figure 4: Synthetic seismograms for a layer-over-halfspace model (Table 2) for several assumptions of thickness. A propagator matrix method was used to compute the impulse response (Haskell, 1962). A simple pulse-like time function and 15-100 instrument response was also included. Major crustal conversions and reverberations are indicated on the bottom trace. Ps is the P to SV conversion at the crust-mantle interface in the model. PpP_mS represents a P wave which passes through the Moho, reflects from the free surface as a P wave and reflects back up from the Moho as an SV wave.

Figure 5: COR crustal model derived in Langston (1977a).

Figure 6: Equilization of radial components from the COR and VIC data.

Figure 7: Data (top) and synthetic seismograms (below) showing the effect of dip on the interface at 45 km depth under COR.

Figure 8: Schematic cross-section along a profile perpendicular to the Oregon coast and including COR. Structures at G11 and G10 are taken from Shor et al (1968).

Figure 9: Preliminary condensed cross-section of the geometry of the subducting Moho under the Pacific Northwest.

Figure 10: Layered model used in calculating the synthetics of Figure 11.

Figure 11: Synthetic refraction profile for distances near the cross-over of the head wave from the 20 km depth interface of the model in Figure 10. Arrival 'A' is the reflection from the 45 km depth interface. Arrival 'B' is the post-critical reflection from the top of the interface at 20 km depth. Arrival 'C' is the post-critical reflection from the interface near 6 km depth.

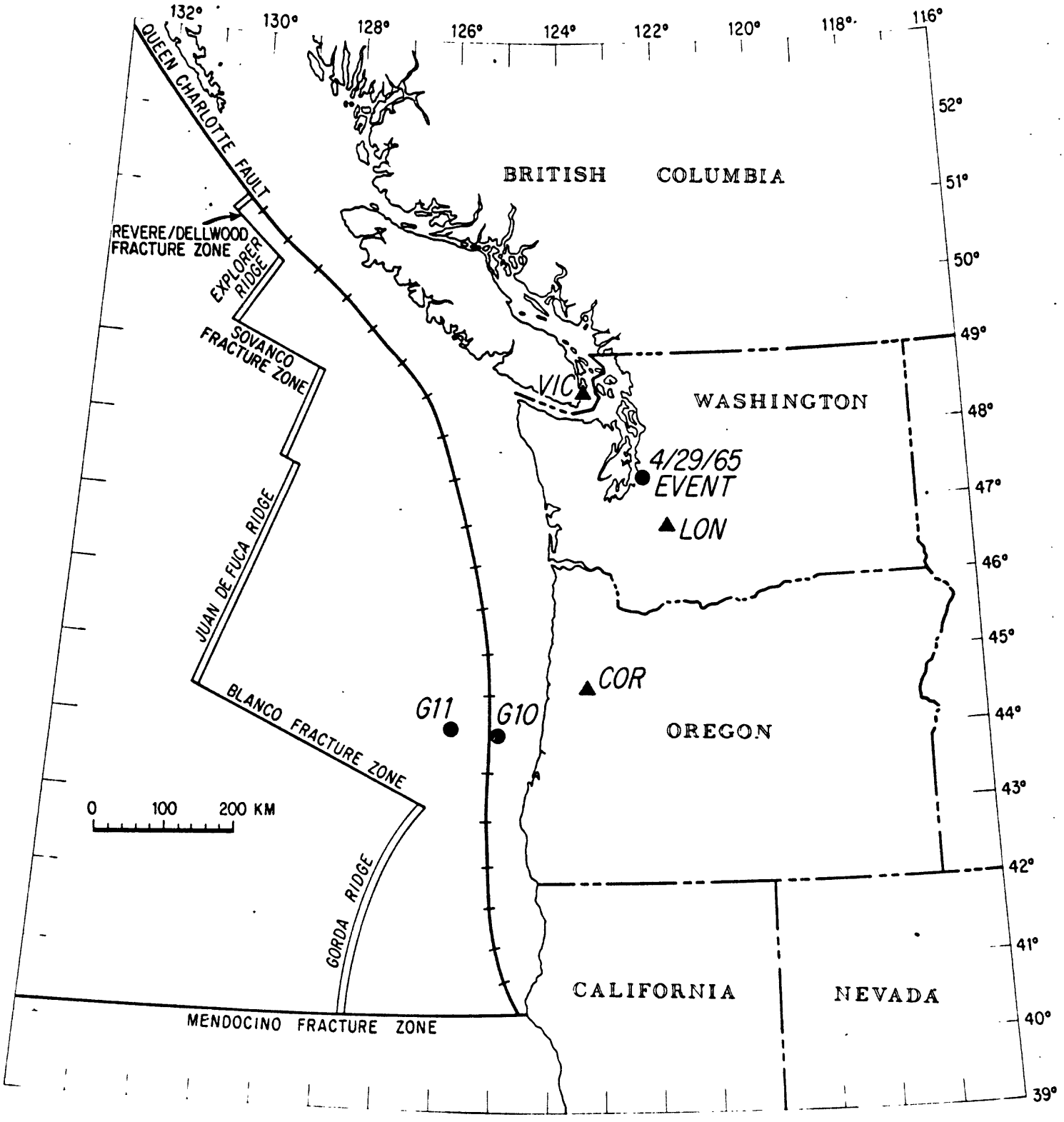
132°
130°
128°
126°
124°
122°
120°
118°
116°
52°
51°
50°
49°
48°
47°
46°
45°
44°
43°
42°
41°
40°
39°
QUEEN CHARLOTTE FAULT
REVERE/DELLWOOD FRACTURE ZONE
EXPLORER RIDGE
SOVANCO FRACTURE ZONE
JUAN DE FUCA RIDGE
BLANCO FRACTURE ZONE
GORDA RIDGE
MENDOCINO FRACTURE ZONE
BRITISH COLUMBIA
WASHINGTON
OREGON
CALIFORNIA
NEVADA
VIC
4/29/65 EVENT
LON
COR
G11
G10
0 100 200 KM

Fig. 1

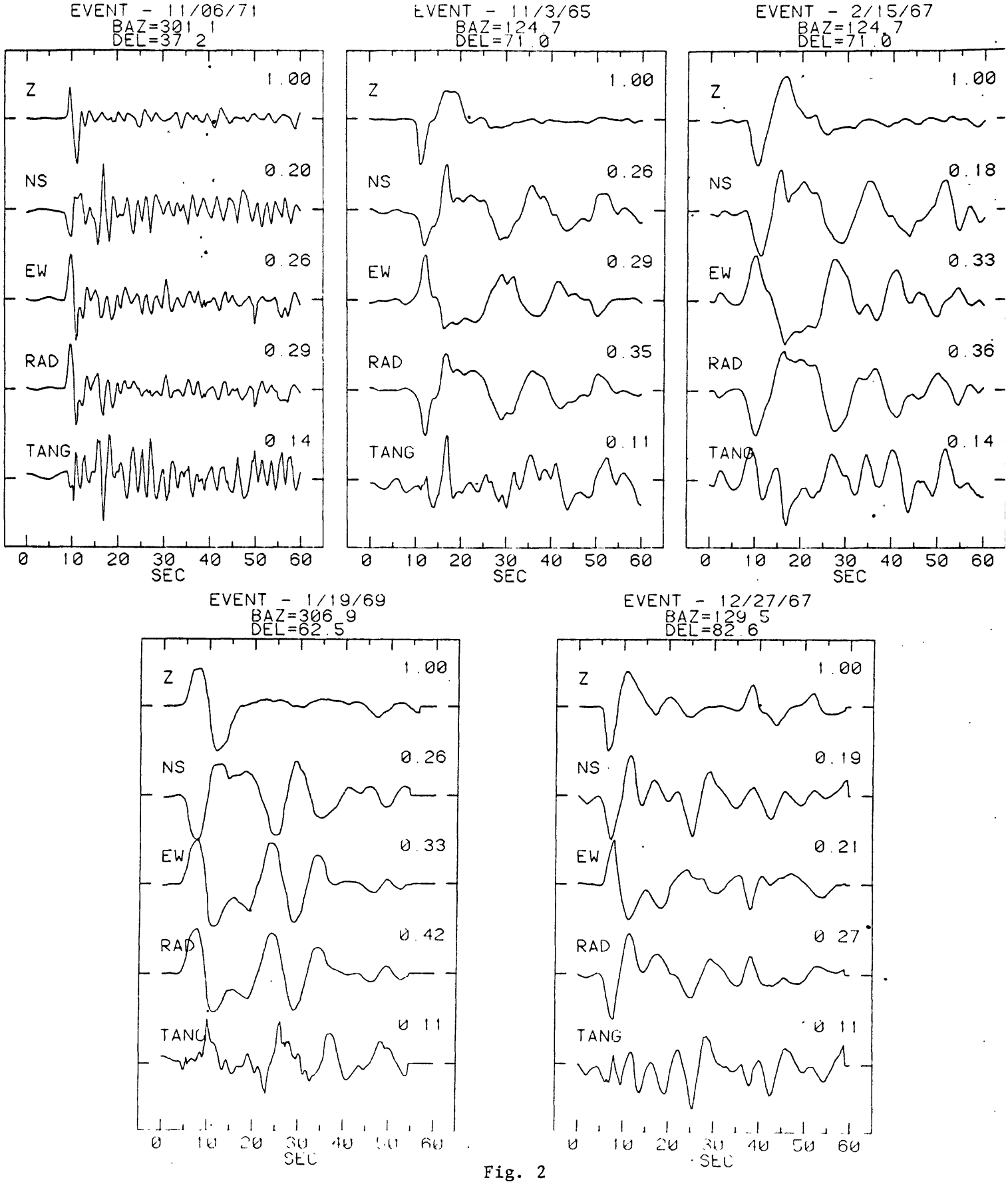
EVENT - 11/06/71
BAZ=301.1
DEL=37.2
Z
1.00
NS
0.20
EW
0.26
RAD
0.29
TANG
0.14
0 10 20 30 40 50 60
SEC
EVENT - 11/3/65
BAZ=124.7
DEL=71.0
Z
1.00
NS
0.26
EW
0.29
RAD
0.35
TANG
0.11
0 10 20 30 40 50 60
SEC
EVENT - 2/15/67
BAZ=124.7
DEL=71.0
Z
1.00
NS
0.18
EW
0.33
RAD
0.36
TANG
0.14
0 10 20 30 40 50 60
SEC
EVENT - 1/19/69
BAZ=306.9
DEL=62.5
Z
1.00
NS
0.26
EW
0.33
RAD
0.42
TANG
0.11
0 10 20 30 40 50 60
SEC
EVENT - 12/27/67
BAZ=129.5
DEL=82.6
Z
1.00
NS
0.19
EW
0.21
RAD
0.27
TANG
0.11
0 10 20 30 40 50 60
SEC

Fig. 2

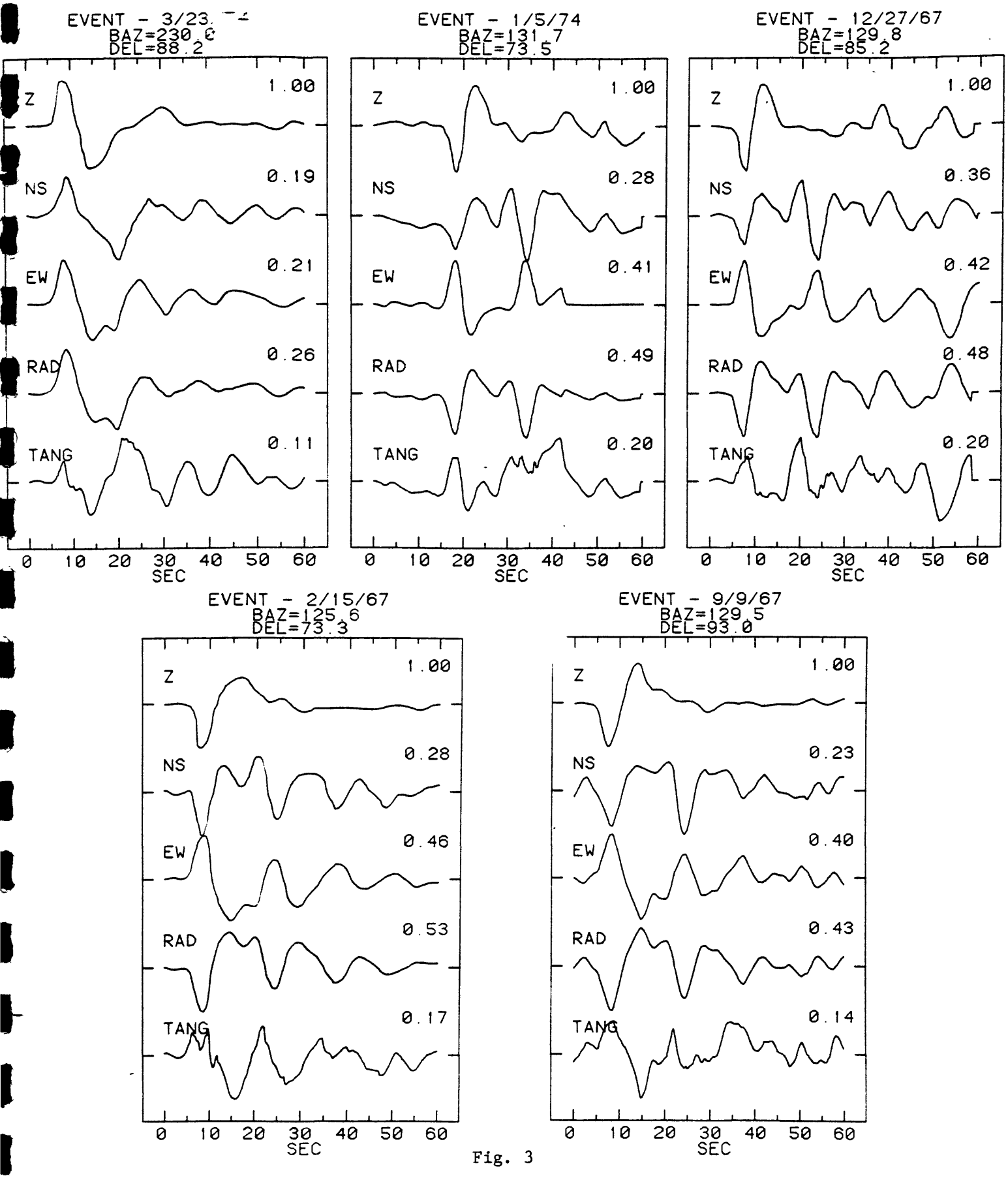
EVENT - 3/23
BAZ=230.6
DEL=88.2
EVENT - 1/5/74
BAZ=131.7
DEL=73.5
EVENT - 12/27/67
BAZ=129.8
DEL=85.2
Z
NS
EW
RAD
TANG
1.00
0.19
0.21
0.26
0.11
1.00
0.28
0.41
0.49
0.20
1.00
0.36
0.42
0.48
0.20
0 10 20 30 40 50 60
SEC
EVENT - 2/15/67
BAZ=125.6
DEL=73.3
EVENT - 9/9/67
BAZ=129.5
DEL=93.0
1.00
0.28
0.46
0.53
0.17
1.00
0.23
0.40
0.43
0.14

Fig. 3

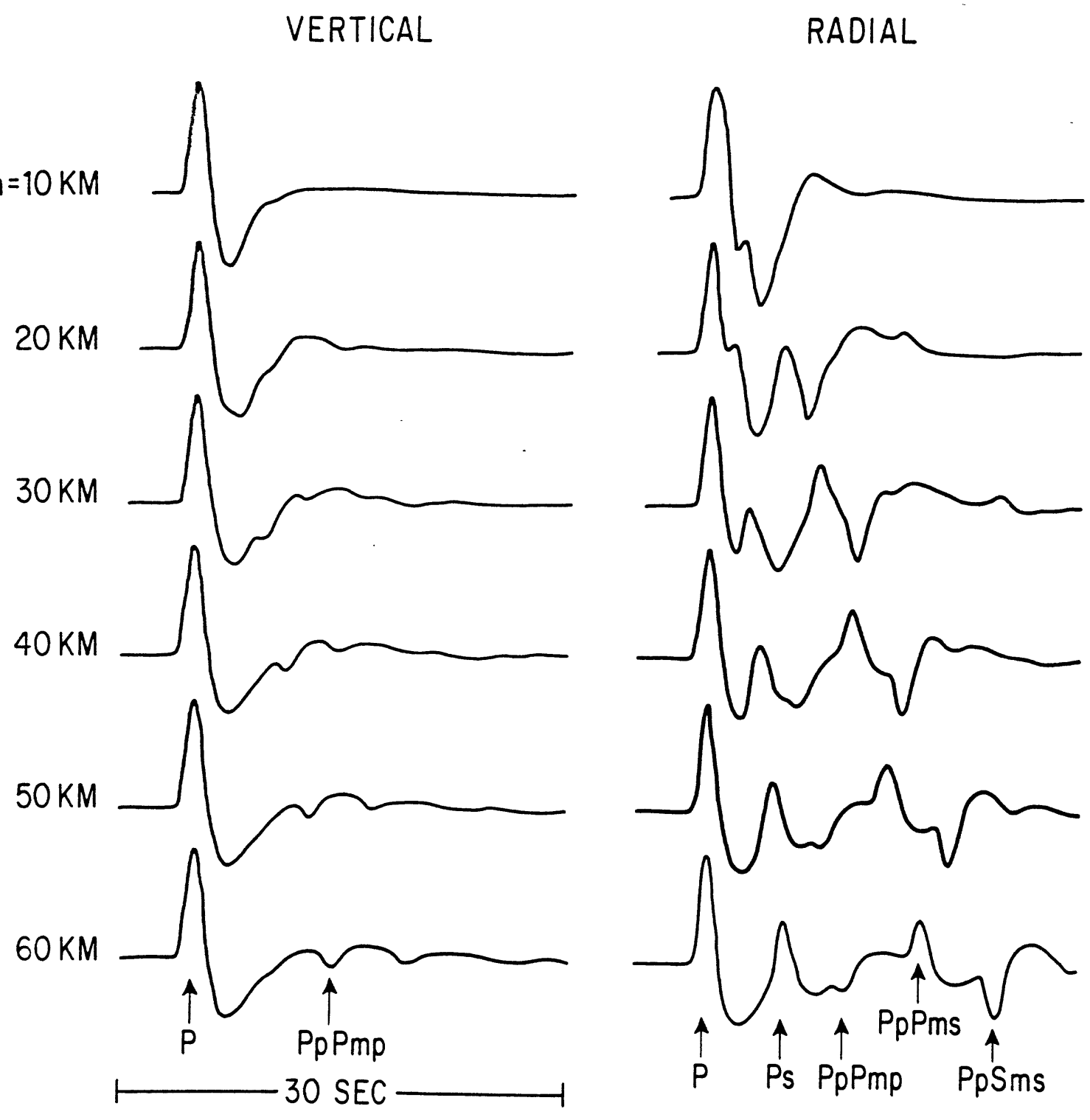
VERTICAL
RADIAL
h=10 KM
20 KM
30 KM
40 KM
50 KM
60 KM
P
PpPmp
30 SEC
P
Ps
PpPmp
PpPms
PpSms

Fig. 4

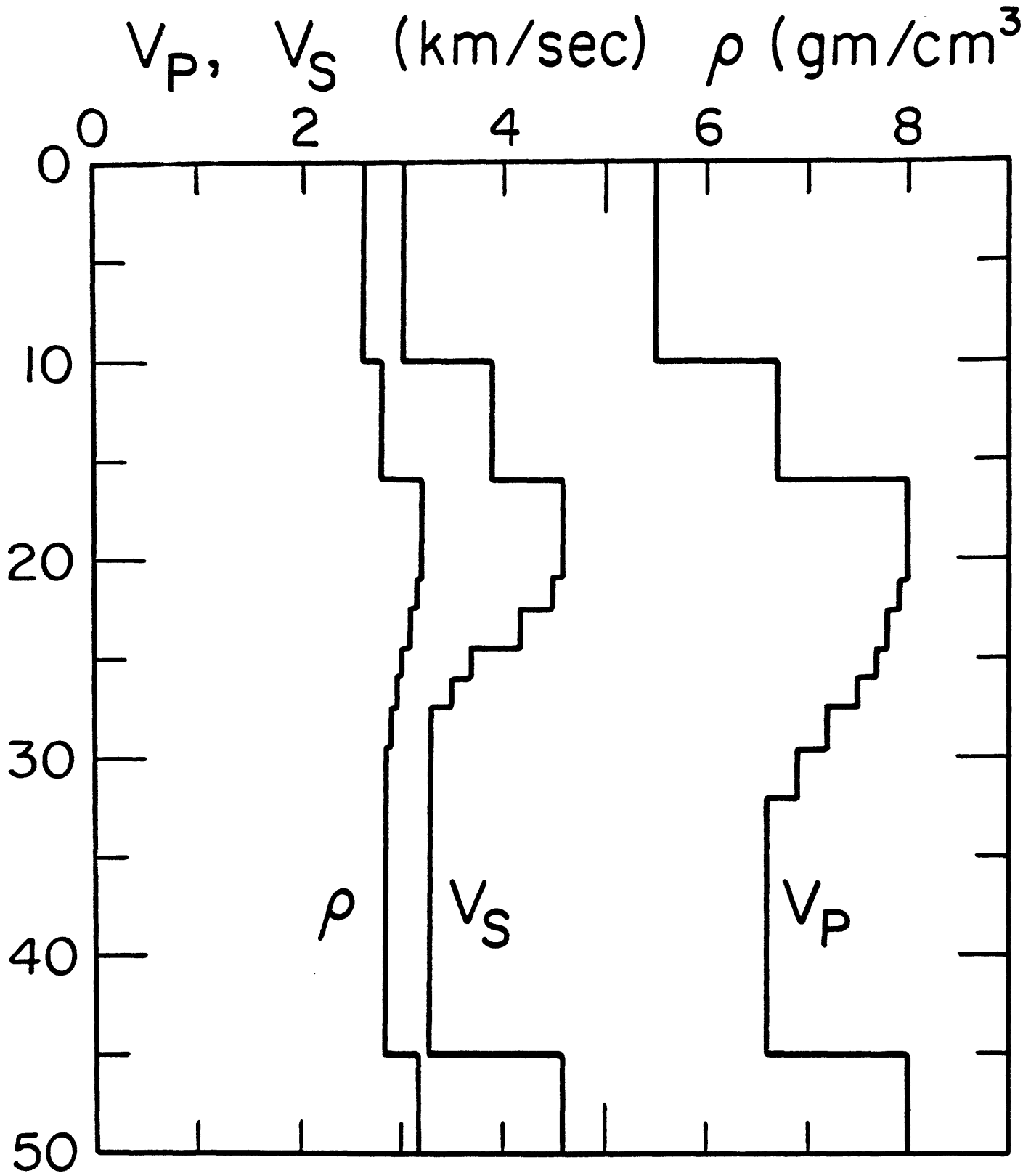

Fig. 5

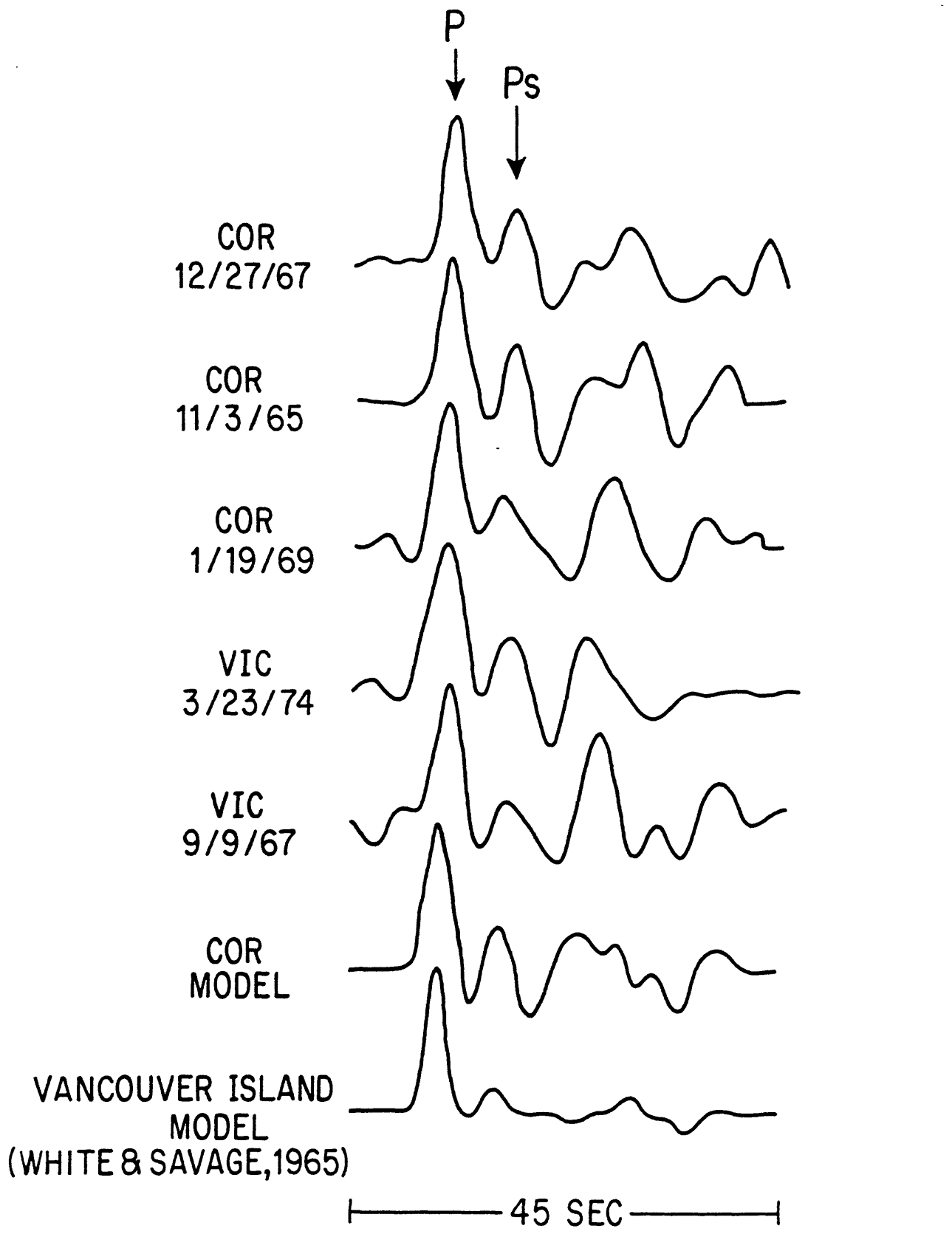
RADIAL COMPONENT DECONVOLUTIONS
P
Ps
COR
12/27/67
COR
11/3/65
COR
1/19/69
VIC
3/23/74
VIC
9/9/67
COR
MODEL
VANCOUVER ISLAND
MODEL
(WHITE & SAVAGE, 1965)
45 SEC

Fig. 6

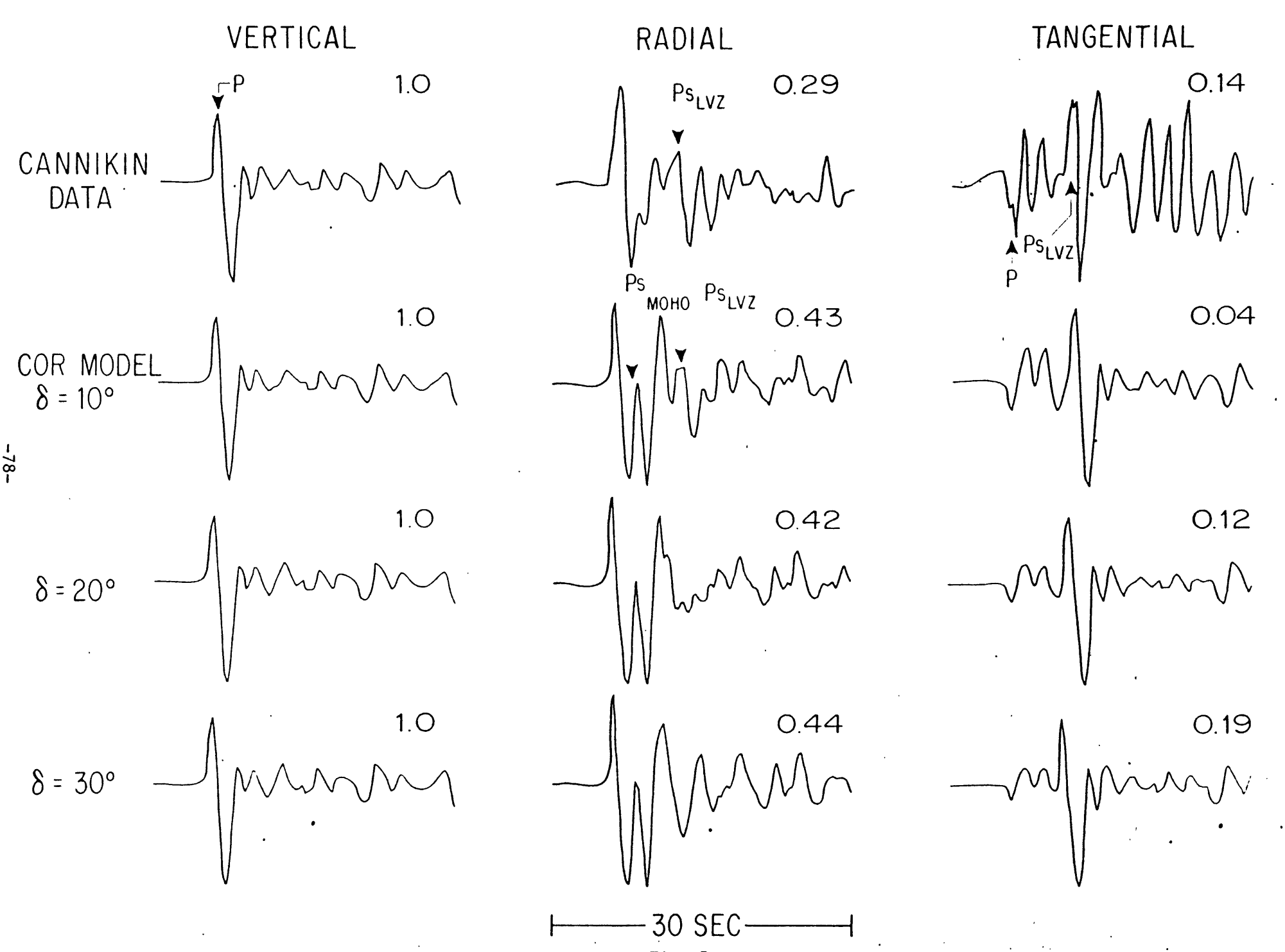
VERTICAL
RADIAL
TANGENTIAL
P
1.0
Ps LVZ
0.29
0.14
CANNIKIN DATA
Ps LVZ
P
Ps MOHO
Ps LVZ
1.0
0.43
0.04
COR MODEL δ = 10°
1.0
0.42
0.12
δ = 20°
1.0
0.44
0.19
δ = 30°
30 SEC

Fig. 7

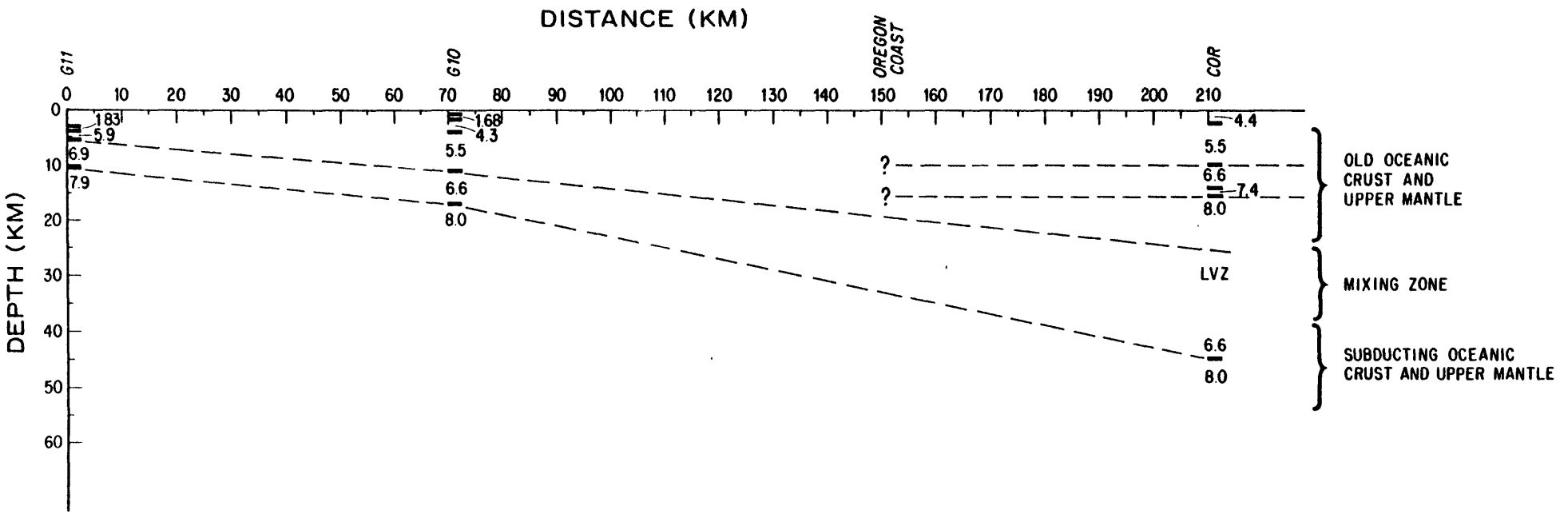
DISTANCE (KM)
G11
G10
OREGON COAST
COR
0 10 20 30 40 50 60 70 80 90 100 110 120 130 140 150 160 170 180 190 200 210
DEPTH (KM)
0 10 20 30 40 50 60
1.83
5.9
6.9
7.9
1.68
4.3
5.5
6.6
8.0
4.4
5.5
?
6.6
?
7.4
8.0
LVZ
6.6
8.0
OLD OCEANIC CRUST AND UPPER MANTLE
MIXING ZONE
SUBDUCTING OCEANIC CRUST AND UPPER MANTLE

Fig. 8

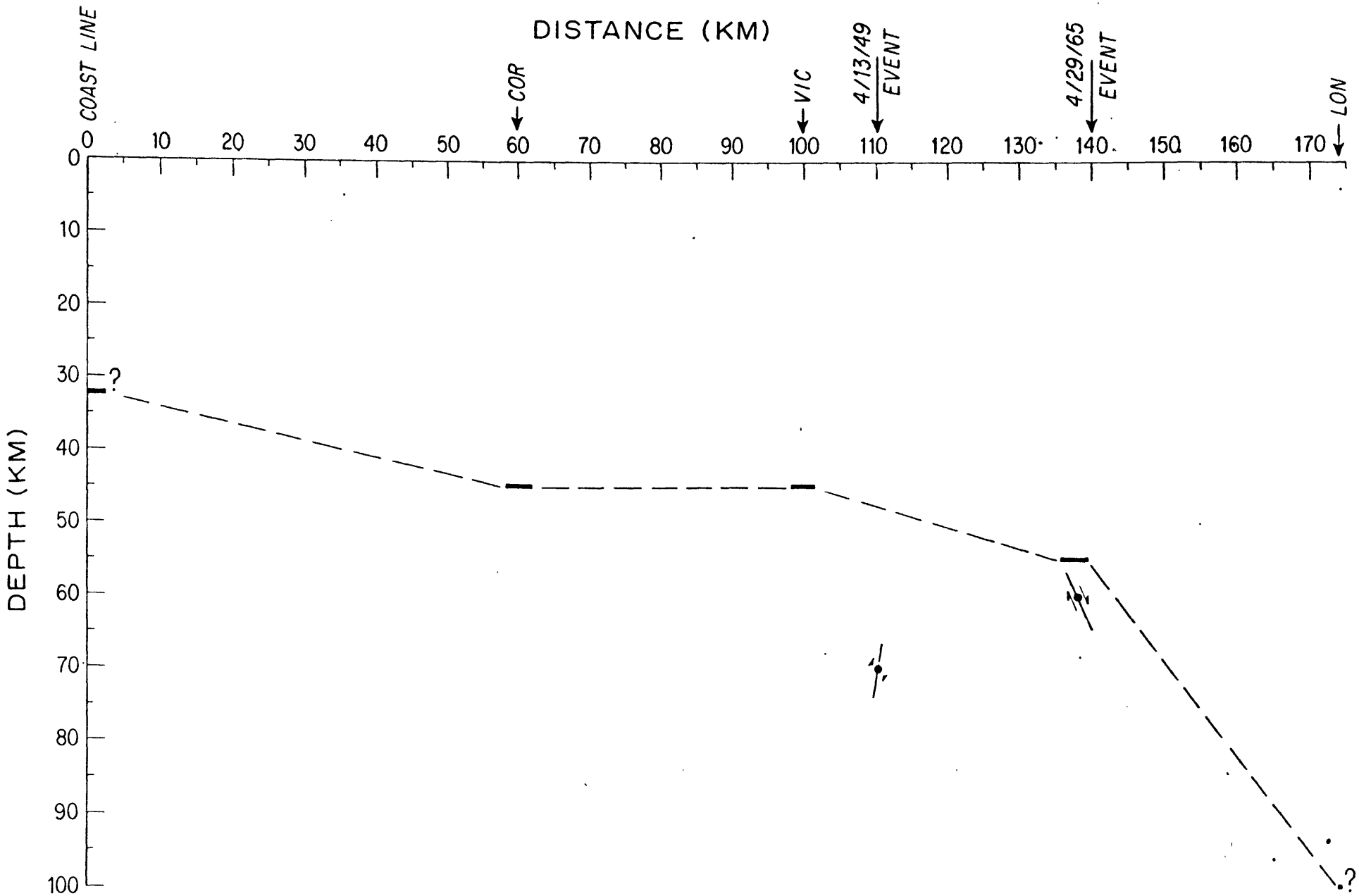
DISTANCE (KM)
COAST LINE
COR
VIC
4/13/49 EVENT
4/29/65 EVENT
LON
0
10
20
30
40
50
60
70
80
90
100
110
120
130
140
150
160
170
DEPTH (KM)
?
?

Fig. 9

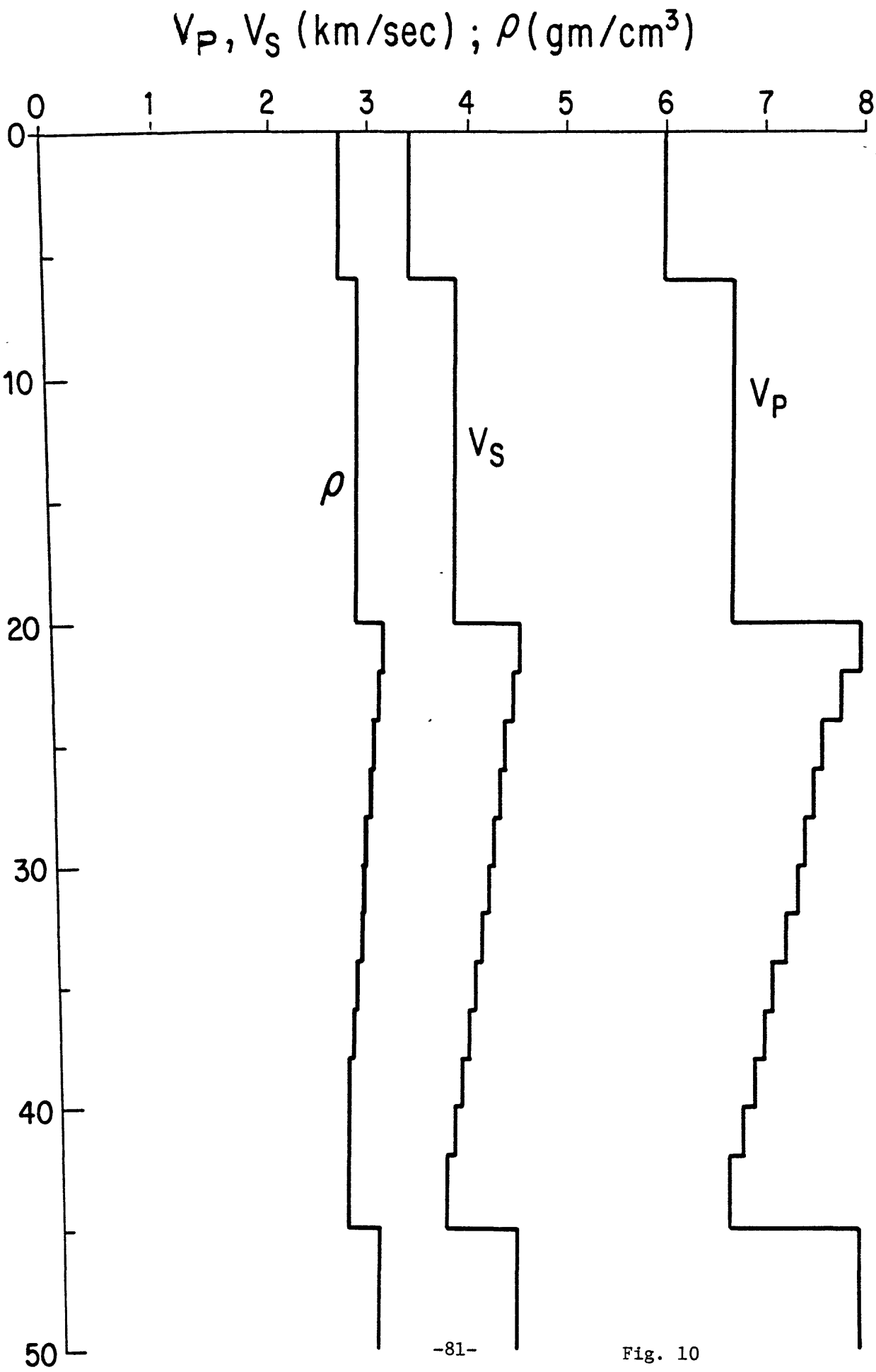

Fig. 10

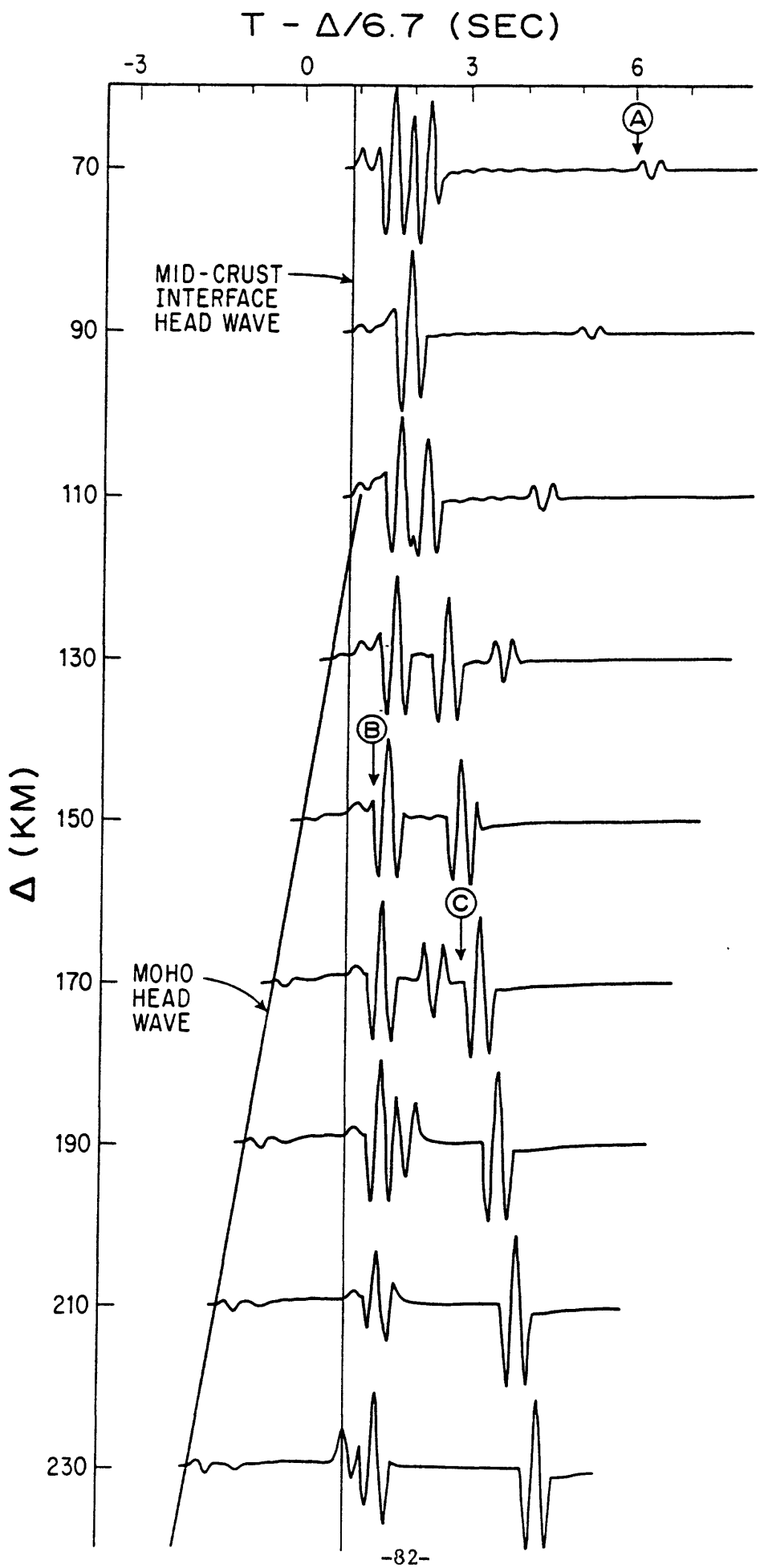
T - Δ/6.7 (SEC)
-3
0
3
6
70
90
110
130
150
170
190
210
230
Δ (KM)
A
B
C
MID-CRUST
INTERFACE
HEAD WAVE
MOHO
HEAD
WAVE

Fig. 11